Hard Magnetic Materials with Reduced Rare-Earth Content

Viorel POP

Babeş-Bolyai University, Faculty of Physics,
400084 Cluj-Napoca, Romania

The Scientific research has been conducted by the group of magnetism at UBB

in collaboration with the following teams:

Olivier Isnard
Institut Néel , CNRS, Université Joseph Fourier, Grenoble, France

Ionel Chicinas
Materials Science and Technology Dept., Technical University of Cluj-Napoca, Romania

Jean Marie Le Breton
Groupe de Physique des Matériaux, Université de Rouen, Saint Etienne Du Rouvray, France

Mihaela Văleanu, Petru Palade, Cristian Teodorescu
National Institute of Material Physics, P.O. Box MG-7, R-76900 Magurele, Bucharest, Romania

With the financial supported of
Romanian Ministry of Education and Research, grant PN-II-ID-PCE-2012-4-0470

Outline

- **Introduction**
- **Mn-Al and Mn-Bi magnetic phases**
- **Nanocomposites magnets=Spring magnets**
- **Conclusions**

Outline

- **Introduction**
- **Mn-Al and Mn-Bi magnetic phases**
- **Nanocomposites magnets=Spring magnets**
- **Conclusions**

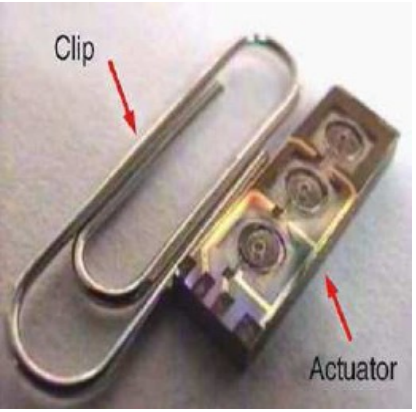

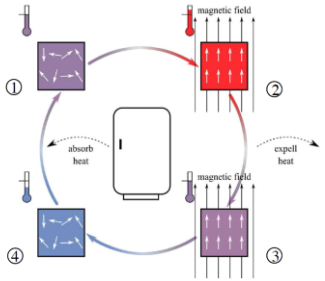

- magnetic materials are ***critical*** components in many devices and for advanced technologies.

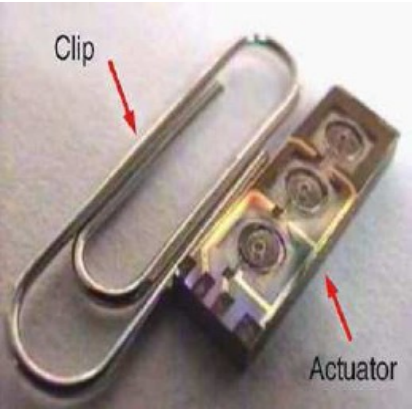

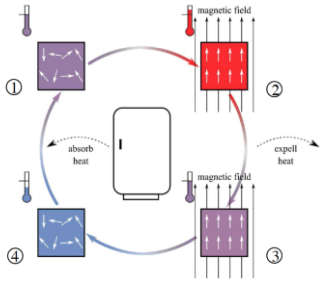

- magnetic materials are ***critical*** components in many devices and for advanced technologies.
- high performance magnet (HPM)/wind generator 1000-1600 kg/MW.
- motors and generators: **2 kg** HPM/hybrid electric vehicle-**20 million** vehicles by 2018.
- Magnetocaloric applications 4 kg HPM/kW cooling power.

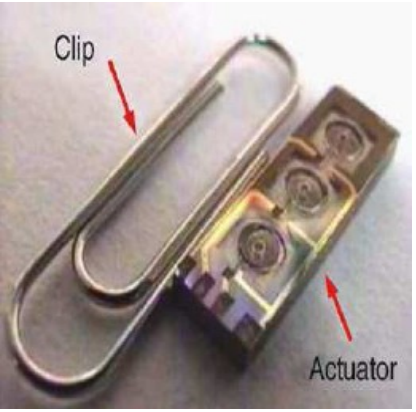

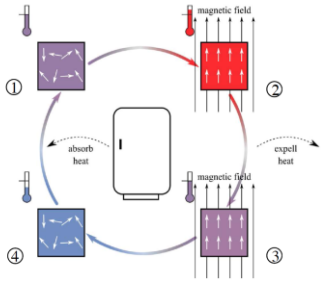

- magnetic materials are ***critical*** components in many devices and for advanced technologies.
- high performance magnet (HPM)/wind generator 1000-1600 kg/MW.
- motors and generators: **2 kg** HPM/hybrid electric vehicle-**20 million** vehicles by 2018.
- Magnetocaloric applications 4 kg HPM/kW cooling power.

HPM= **rare-earth** based magnets

China manages about 96 % of rare-earth resources in 2011

!!!

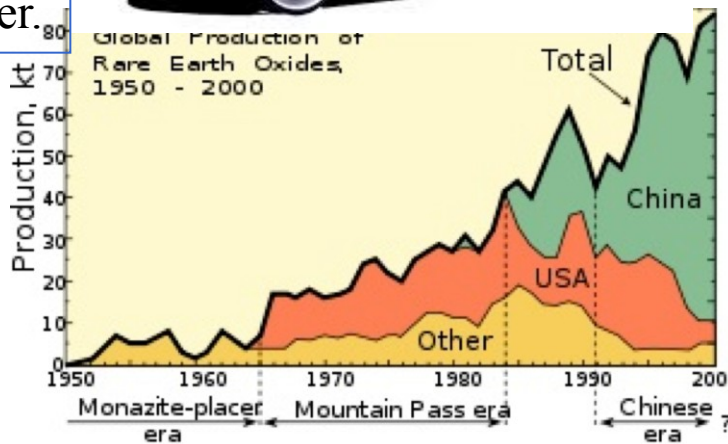

REE price fluctuations*

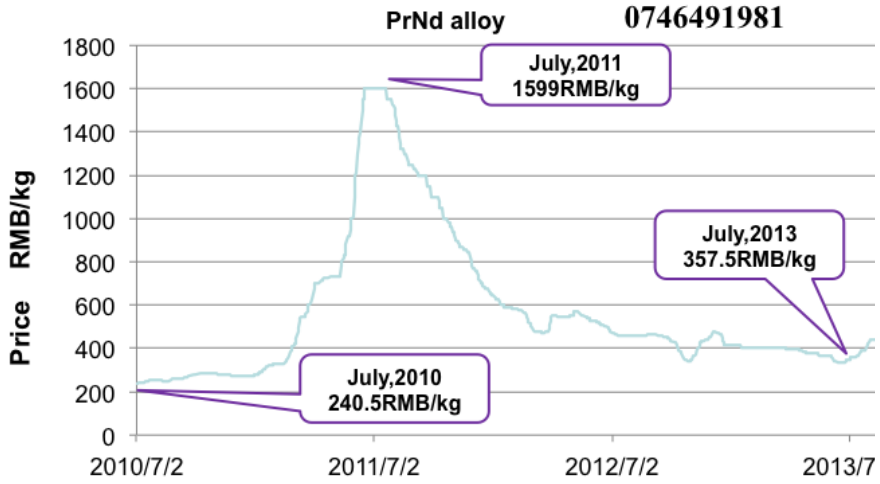

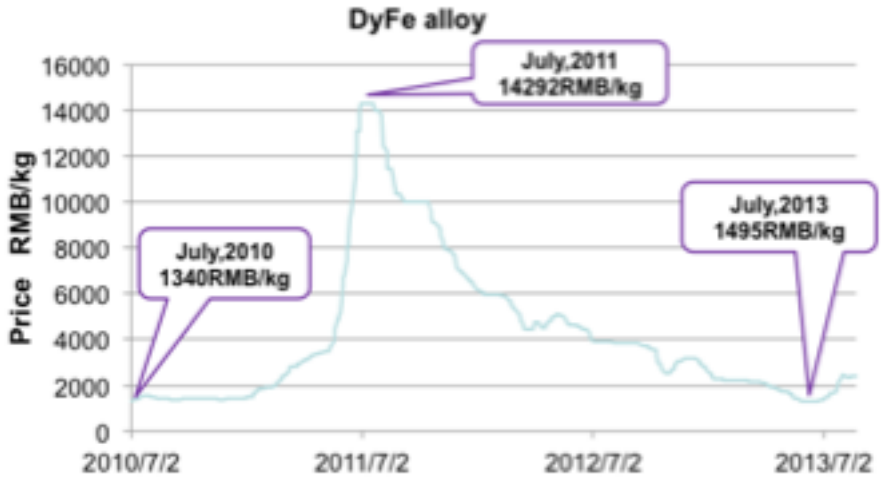

The price of **PrNd** alloy have increased about 565% form November 2010 to July 2011. In July 2013, it drop to 22.4% compare with top price.

The price of **DyFe** alloy have increased about 967% form July 2010 to July 2011. In July 2013, it drop to 10.46% compare with top price.

Instability of RE market, ex. Nd: 150 $/kg/2013; 450 $/kg/2011, 15 $/kg/2009

*Kaihong Ding - *Yantai Shougang Magnetic Materials, China*, Energy and Materials Criticality Workshop, Santorini 2013

Why PM motors?

efficiency **volume** **weight**

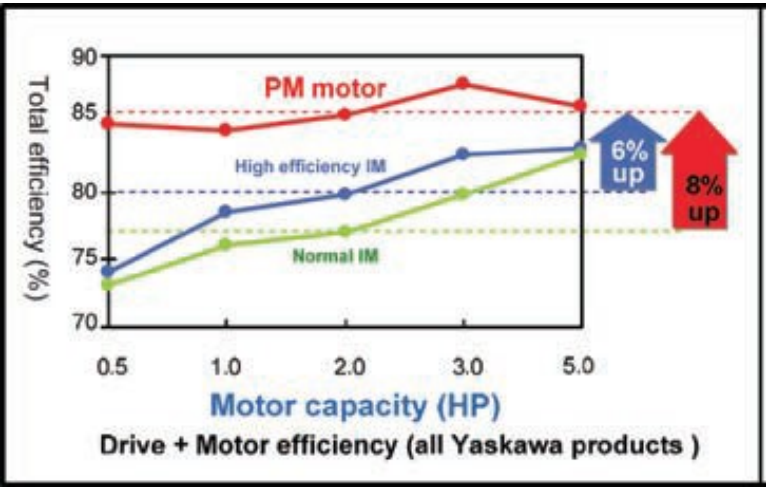

Drive + Motor efficiency (all Yaskawa products)

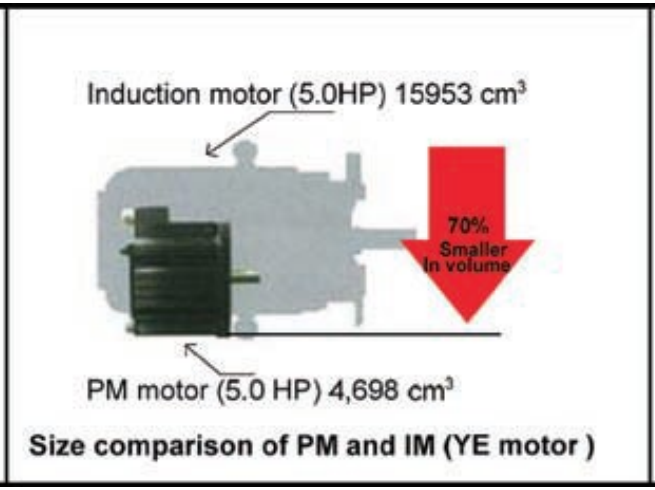

Size comparison of PM and IM (YE motor)

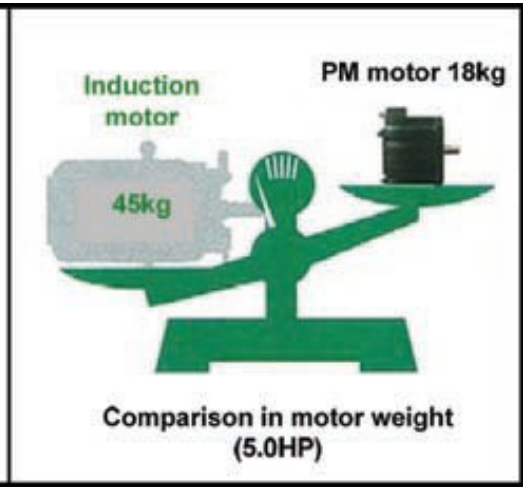

Comparison in motor weight (5.0HP)

*Gutfleisch et al. Adv. Mater. 23 (2011) 821–842

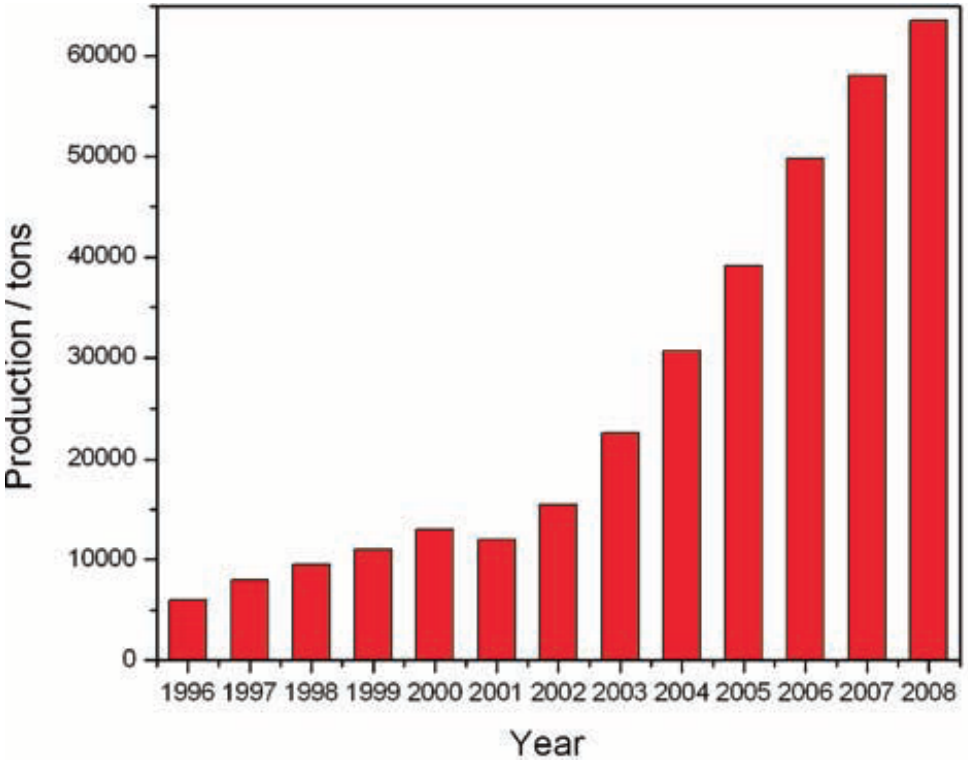

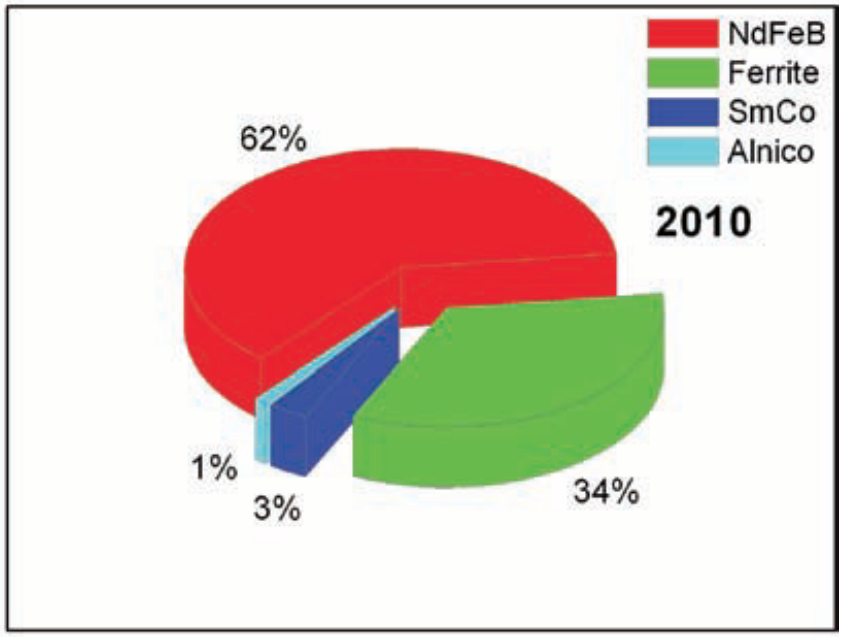

Output of NdFeB permanent magnets during the past ten years (left) [1]
Percentage sales ($) for 2010 of the major permanent magnets in the world (right) [2]*.
**Gutfleisch et al. Adv. Mater. 23 (2011) 821–842.*

[1] Yang Luo , Proc. 20 th Int. Workshop on Rare Earth Permanent Magnets and Their Applications , (Ed: D. Niarchos), 2008 , 27 .
[2] US Magnetic Materials Association, http://www.usmagnetmaterials.com/documents/usmma-presentation general-5-08.ppt, (accessed September 2010).

Solutions ?

Solutions ?

Yes, we have to find solutions !

Solutions ?

Yes, we have to have solutions !

1. The increase of usage efficiency.
2. Recycling.

Solutions ?

Yes, we have to have solutions !

1. The increase of usage efficiency.
2. Recycling.
3. ***New magnetic phases*** without rare-earth with high magnetic properties for applications as permanent magnets and magnetic refrigeration.: Fe-Co and Fe-Ni tetragonal, Fe-Co ternary or quaternary, $Fe_{16}N_2$, MnBi, MnAl, Mn_3Ga, Heusler alloys
4. Soft/hard nanocomposite magnets ➔ ***Spring magnets***

3. ***New magnetic phases*** without rare-earth with high magnetic properties for applications as permanent magnets and magnetic refrigeration.: Fe-Co and Fe-Ni tetragonal, Fe-Co ternary or quaternary, $Fe_{16}N_2$, MnBi, MnAl, Mn_3Ga, Heusler alloys

4. Soft/hard nanocomposite magnets ➔ ***Spring magnets***

The complementary expertise and advanced techniques are required to develop magnets

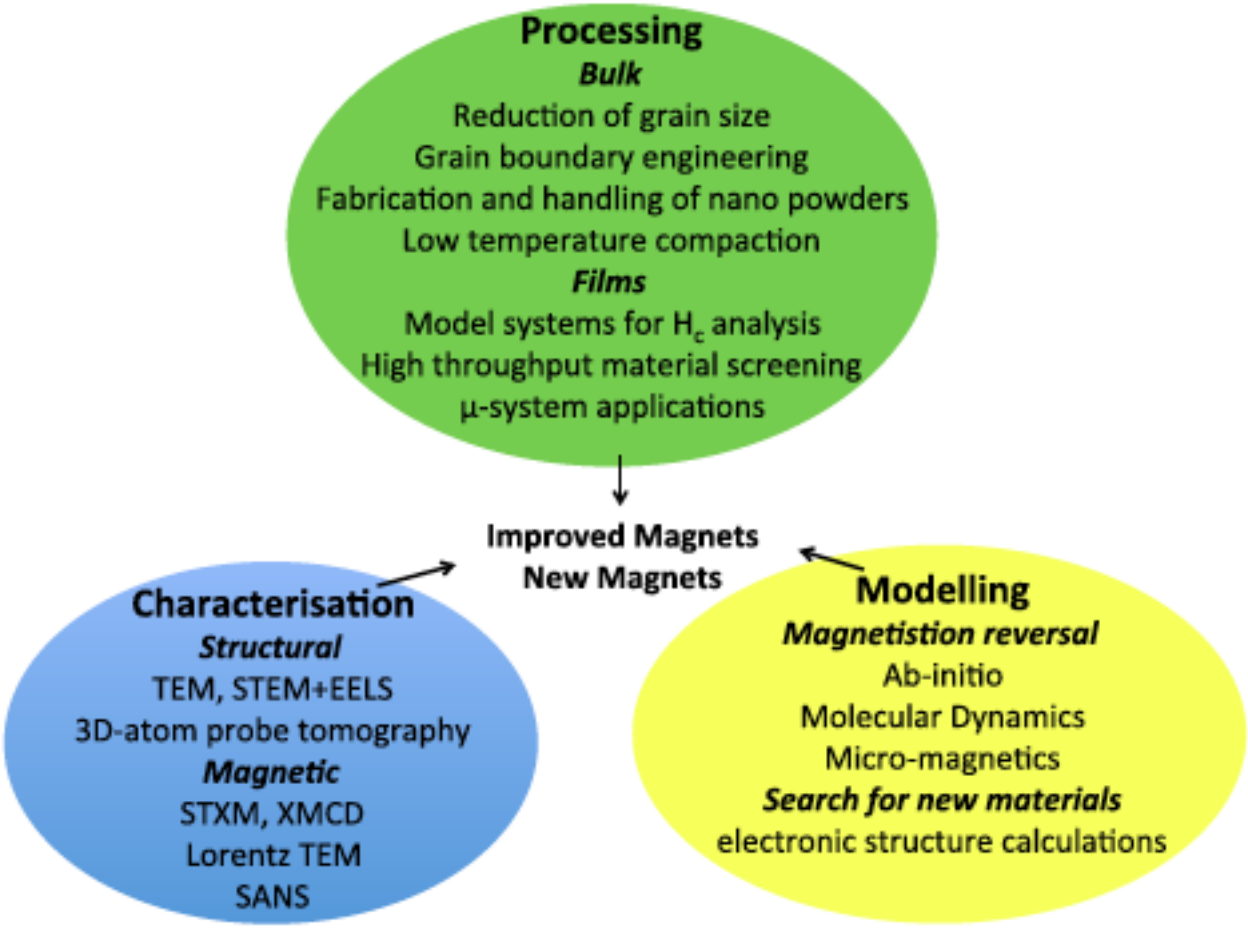

Nora M Dempsey et al, J. Phys. D: Appl. Phys. 47 (2014) 333001

Our recent research in these directions

1. ***New magnetic phases*** without rare-earth with high magnetic properties

2. **Soft**/**hard** nanocomposite magnets ➔ ***Spring magnets***

Our recent research in these directions

1. ***New magnetic phases*** without rare-earth with high magnetic properties

   - ✓ ***MnBi***
   - ✓ ***MnAl***
     - $Mn_{50+\delta}Al_{50-\delta}$; δ=4
     - $Mn_{50}Al_{50-\delta}X_{\delta}$; δ=4, X=Ni, Zn, Ti

2. **Soft/hard** nanocomposite magnets ➔ ***Spring magnets***

   - ✓ **hard magnetic phases of $SmCo_5$, $SmCo_3Cu_2$, $R_2Fe_{14}B$**

   - ✓ **soft magnetic phases of α-Fe, Fe-Co (~20 or 10 wt%)**

Our recent research in these directions

1. ***New magnetic phases*** without rare-earth with high magnetic properties

   - ✓ ***MnBi***
   - ✓ ***MnAl***
     - $Mn_{50+\delta}Al_{50-\delta}$; δ=4
     - $Mn_{50}Al_{50-\delta}X_{\delta}$; δ=4, X=Ni, Zn, Ti

2. **Soft/hard** nanocomposite magnets ➔ ***Spring magnets***

   - ✓ **hard magnetic phases of $SmCo_5$, $SmCo_3Cu_2$, $R_2Fe_{14}B$**
     - **$SmCo_5$** **large anisotropy**
     - **$SmCo_3Cu_2$** **large coercivity**
     - **$R_2Fe_{14}B$** **best magnets**
   - ✓ **soft magnetic phases of α-Fe, Fe-Co (~20 or 10 wt%)**

Outline

- Introduction
- **Mn-Al and Mn-Bi magnetic phases**
- Nanocomposites magnets=Spring magnets
- Conclusions

MnBi magnetic phase

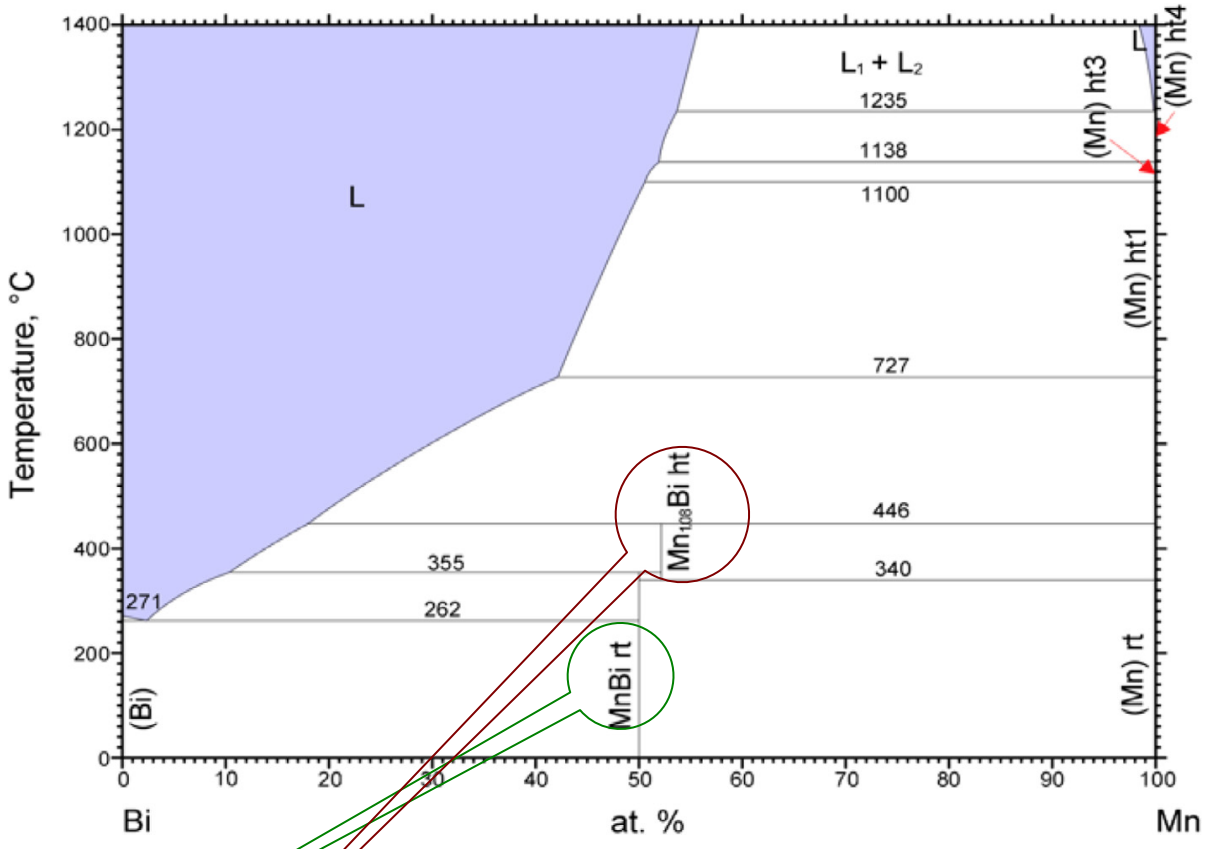

- **Low temperature phase (LTP)-*NiAs type Hexagonal (Ferromagnetic)***
- High temperature phase (HTP) -*Distorted Ni_2In type hexagonal (paramagnetic)*

MnBi magnetic phase

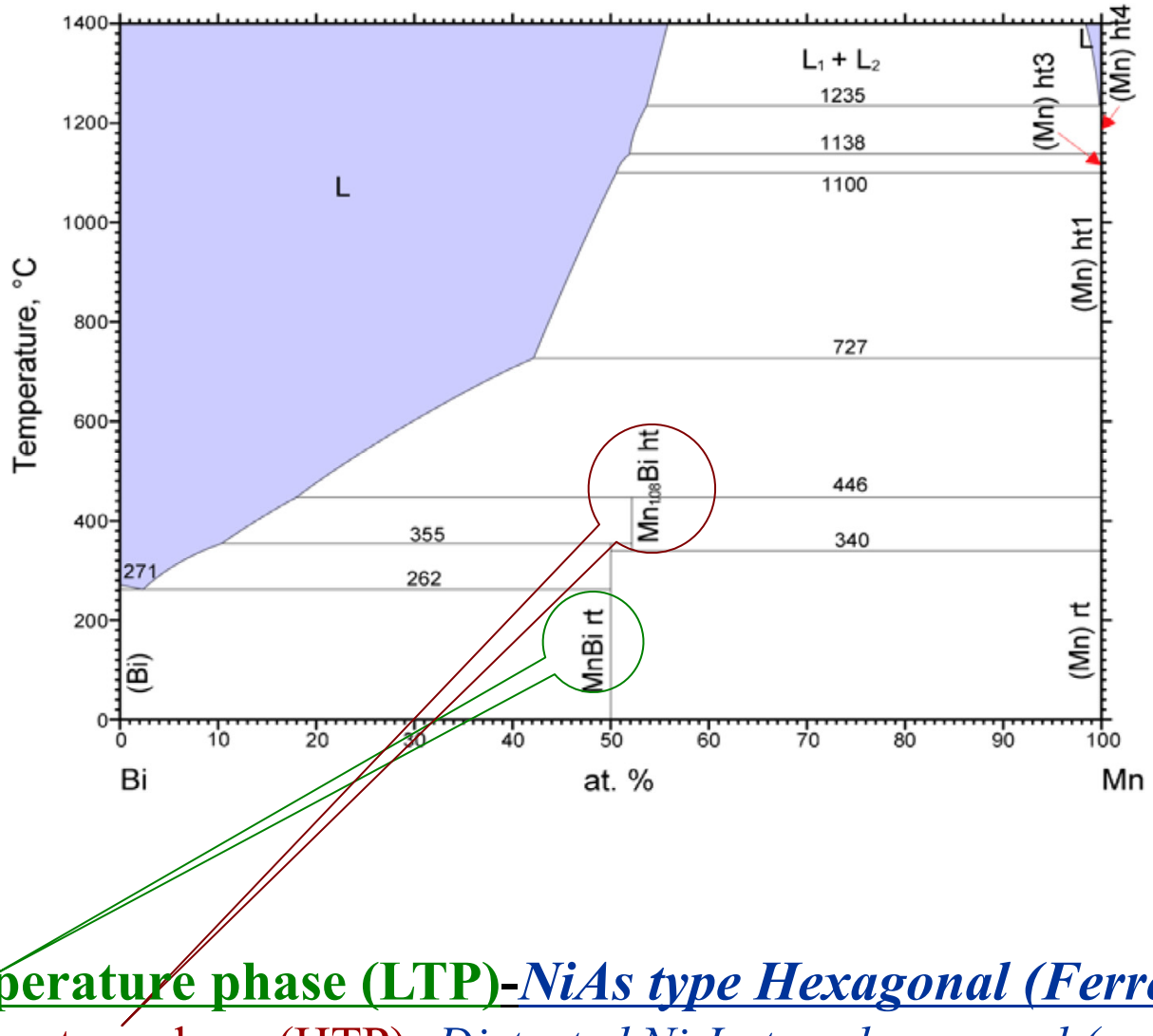

- **Low temperature phase (LTP)-*NiAs type Hexagonal (Ferromagnetic)***
- High temperature phase (HTP) -*Distorted Ni_2In type hexagonal (paramagnetic)*
- Quenched high temperature phase *(QHTP)-Orthorhombic (Ferromagnetic-low M_s)*

Some previous works in MnBi magnetic compound*

Powders: Sintered method & magnetic separation

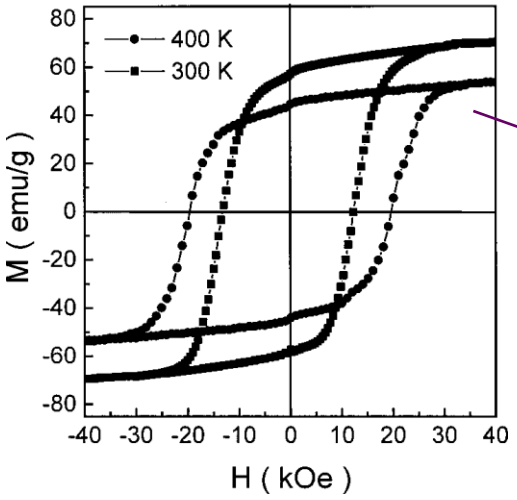

$(BH)_{max}$=7.7 MGOe
(powders)

J B Yang et al. J. Phys.: Condens. Matter 14 (2002) 6509

Nanocrystalline MnBi by melt-spinning technique

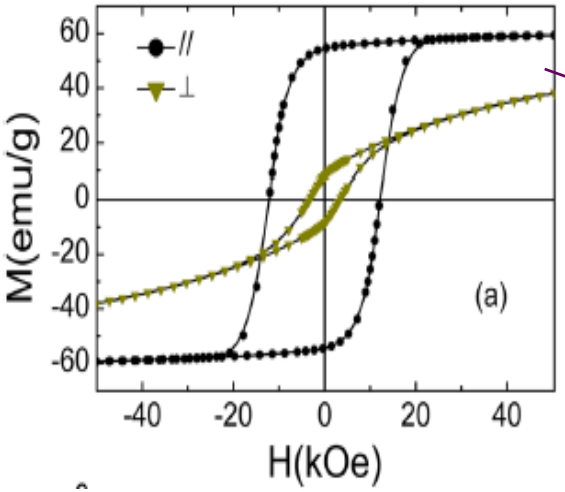

$(BH)_{max}$ = 7.1 MGOe
(powders of melt-spun ribbons)

Yang et al. Appl. Phys. Lett. 99, 082505 (2011)

Hot pressed bulk magnet

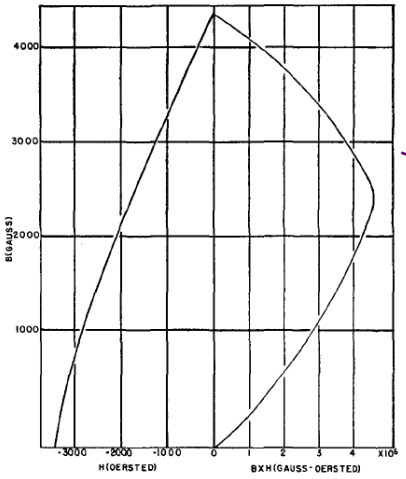

$(BH)_{max}$=4.3 MGOe

Density: 90%

Adams et al. J. Appl. Phys. 23 1207 (1952)

Spark plasma sintered bulk magnet

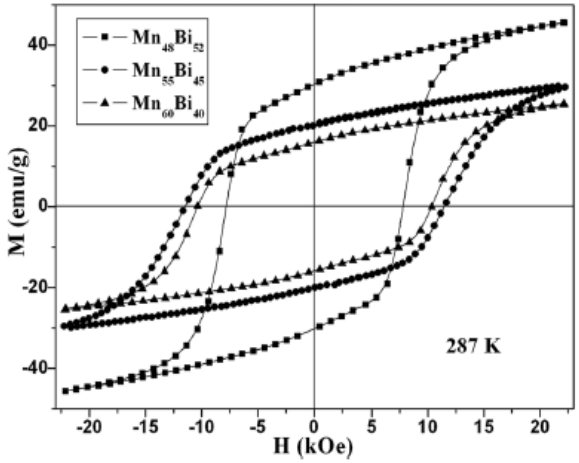

$(BH)_{max}$< 2 MGOe

Density: 93%

Zhang et al. J. Appl. Phys 109, 07A722 (2011)

*G. Hadjipanayis, Delaware University, Energy and Materials Criticality Workshop, Santorini 2013

J. Cui et al. / Acta Materialia 79 (2014) 374–381

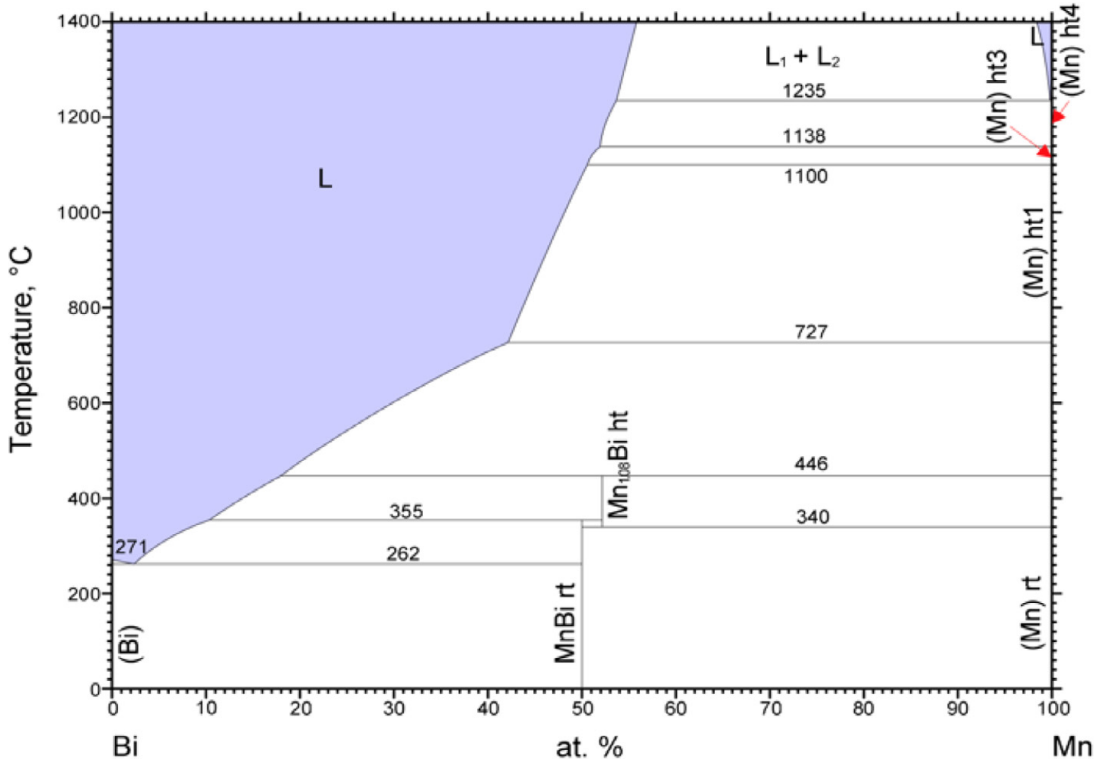

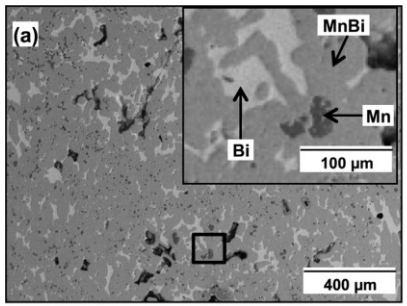

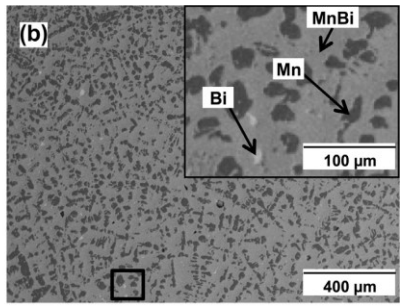

Difficulty of obtaining a high volume fraction of the **desired LTP MnBi**, originated from the **peritectic** formation of MnBi LTP and hence **Mn and Bi tends to precipitate out** of the MnBi liquid during the solidification process

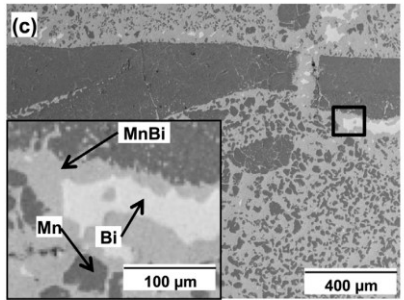

Our main results

MnBi

Synthesis:

- ✓ melting : Mn and Bi of 99,99% purity (1 wt % Mn in excess)
- ✓ annealing : 258-420ºC/ from 2 hours to 4 days
- ✓ mechanical milling: of bulk MnBi phase for 2 hours

X-rays powder diffraction:

- ✓ K_{α} radiation of copper in the angular range 2θ = 20 - 100° and
- ✓ $K_{\alpha 1}$ radiation of cobalt in angular range 2θ= 20 - 80º

Magnetic measurements:

- ✓ extraction method in a continuous magnetic field of up to ± 10 T

MnBi: influence of ***annealing***

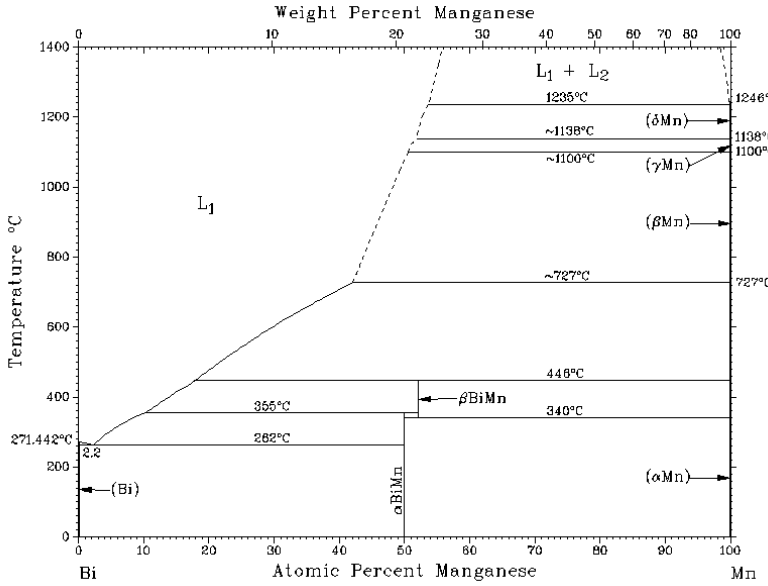

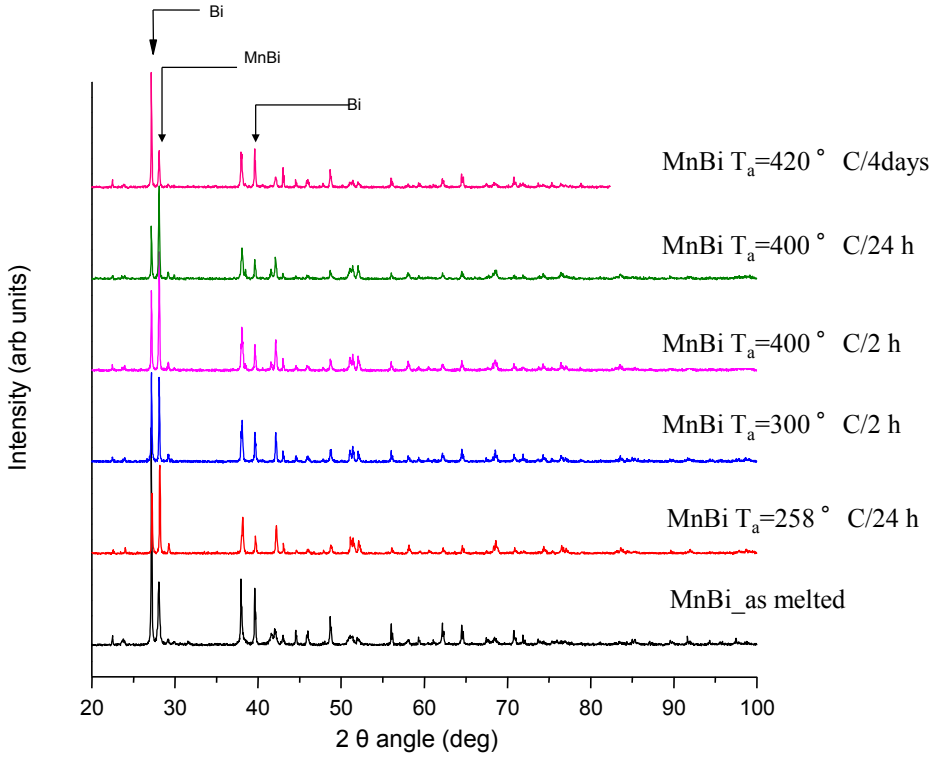

MnBi: influence of ***annealing***; XRD Cu K_α radiation

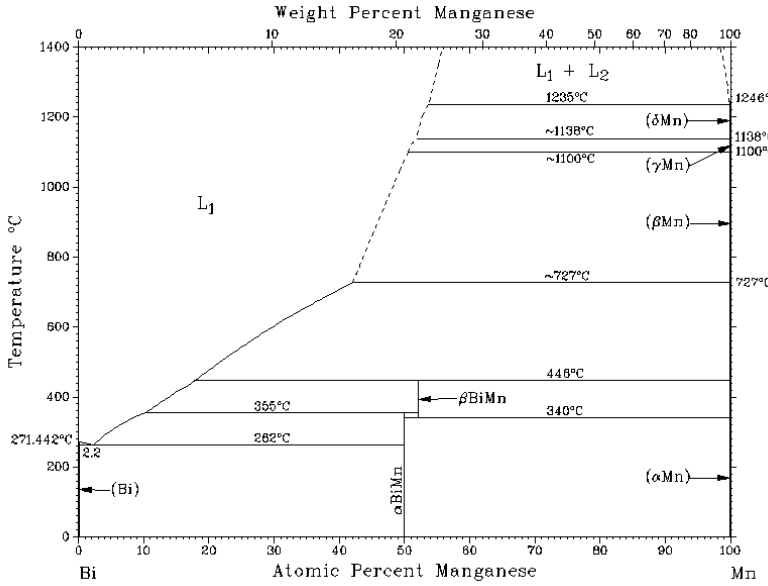

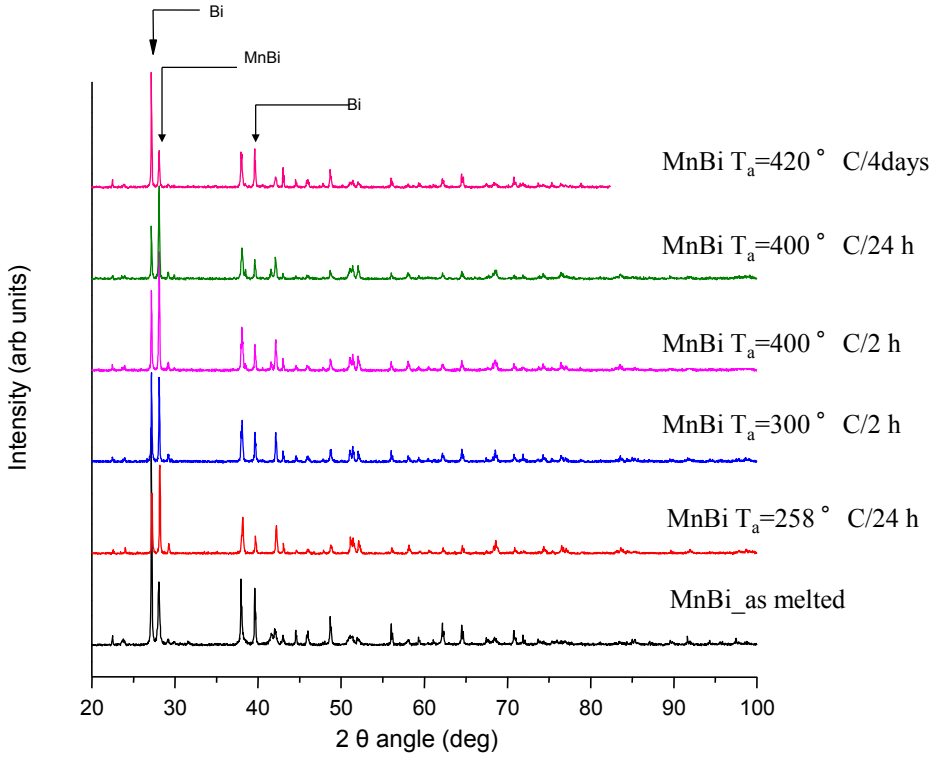

MnBi: influence of ***annealing***; XRD Cu K_α radiation

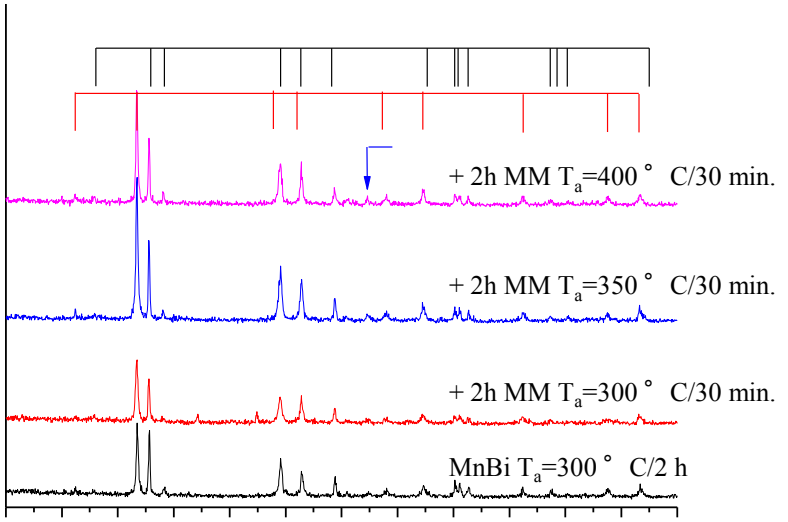

MnBi: influence of ***milling***; XRD Co K_α radiation

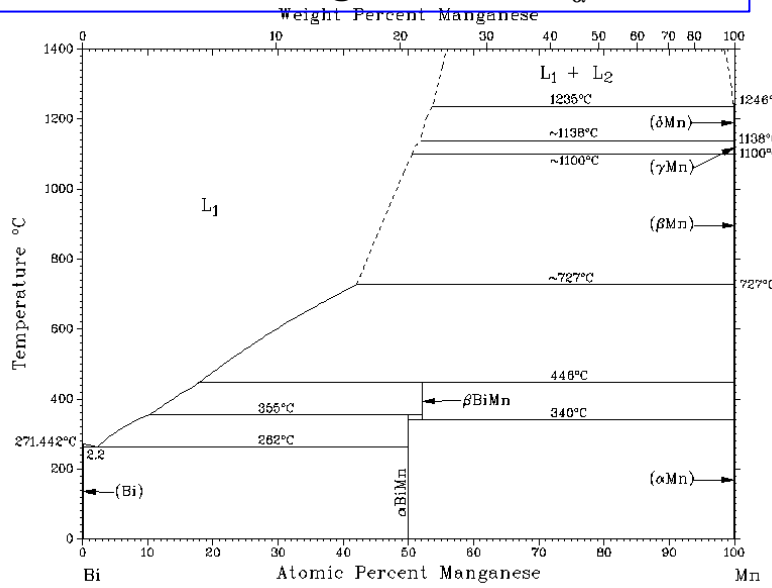

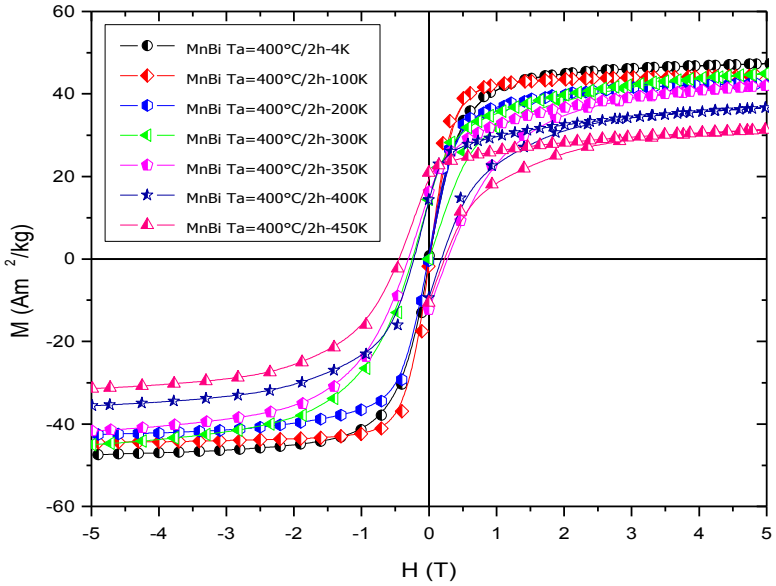

M(H) for different T,
MnBi melted samples, annealed at 400ºC for 2 h

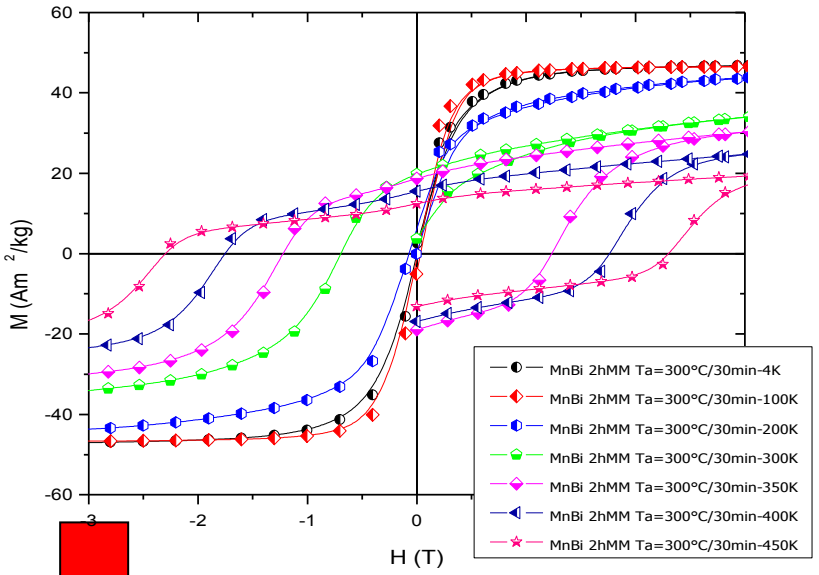

Hysteresis loops for different T,
MnBi 2h MM+TT 300 ºC/30 min

Important coercivity at high temperature, competition with REPM

M. S. Gutoiu, E. Dorolti, O. Isnard, V. Pop, I. Chicinaş, Studia Univ. "Babes-Bolyai", Physica, 54 (2009) 33

Mn-Al magnetic phase

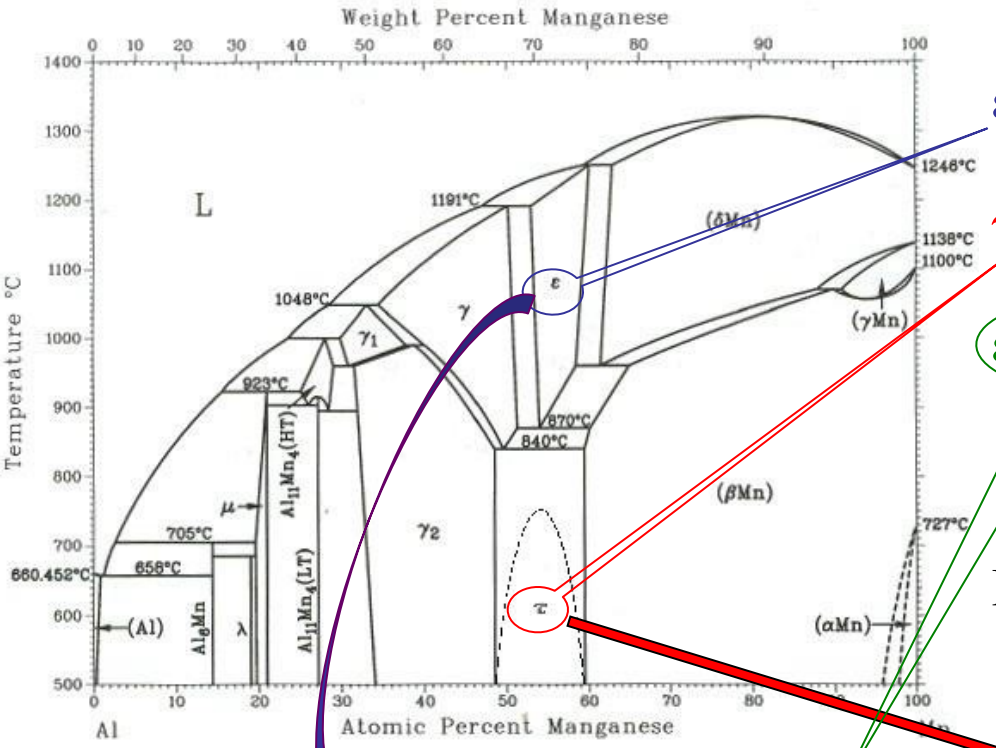

ε phase –
antiferromagnetic hexagonal structure

τ phase –
$L1_0$- ferromagnetic tetragonal structure

ε' phase –
Intermediate ferromagnetic ***ordered*** orthorhombic phase

$Mn_{54}Al_{46}$- the best results

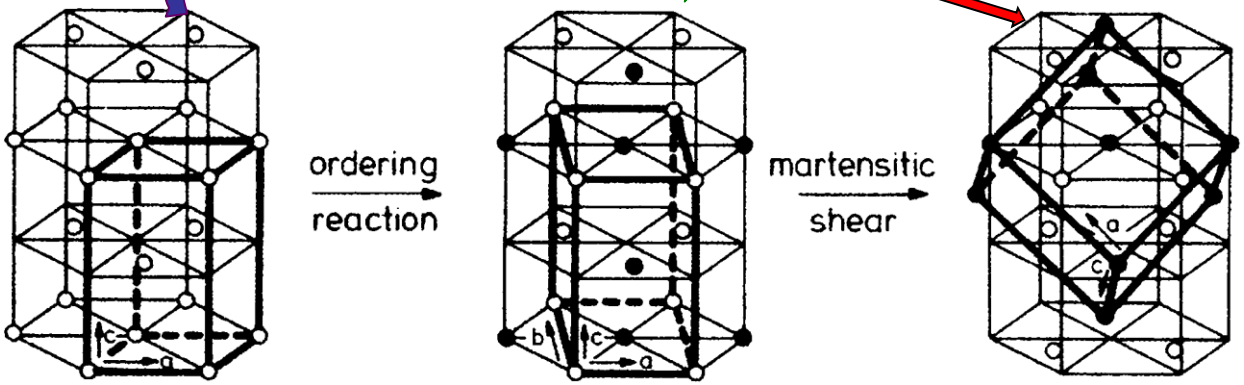

- Phase transformation proposed by Broek et. al. with intermediate ordered orthorhombic phase (B19) denoted by ε'.
- Acta Metall.,27(1979) 1497

Phase formation, microstructure, magnetic properties of the Mn–Al–C; bulk or MM*

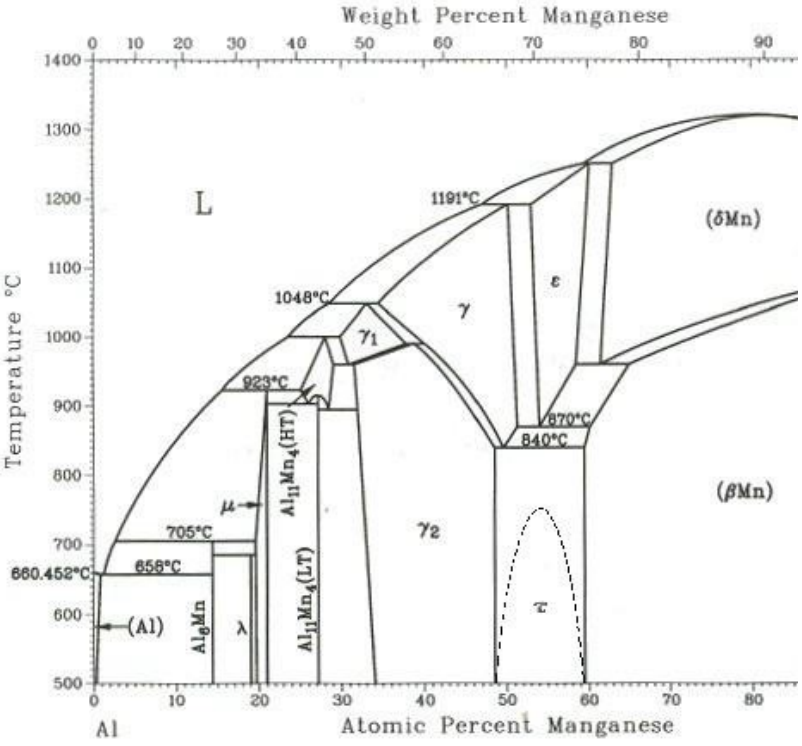

- DSC: the transformation **ε(ε')➔ τ phase**,
- **τ** –phase stabilized by C doping,
- C doping *cannot prevent* the formation of the equilibrium phases from the metastable ε -phase during annealing.

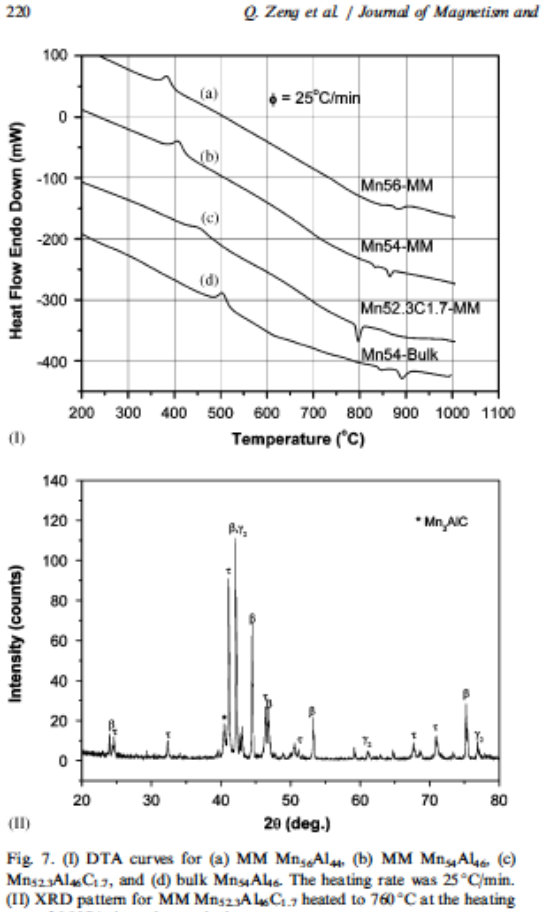

Fig. 7. (I) DTA curves for (a) MM $Mn_{56}Al_{44}$, (b) MM $Mn_{54}Al_{46}$, (c) $Mn_{52.3}Al_{46}C_{1.7}$, and (d) bulk $Mn_{54}Al_{46}$. The heating rate was 25 °C/min. (II) XRD pattern for MM $Mn_{52.3}Al_{46}C_{1.7}$ heated to 760 °C at the heating rate of 25 °C/min and quenched.

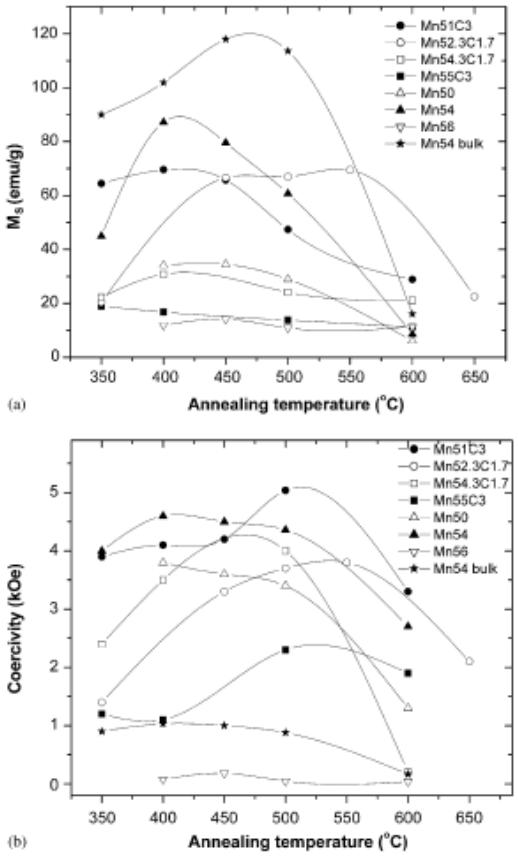

Fig. 8. Dependence of M_S and H_C on the annealing temperatures for MM and bulk samples with various compositions as indicated. The annealing time was 30 min.

The optimal magnetic properties for the MM samples, H_c=4.8 kOe, M_r=45 emu/g and M_s= 89 emu/g, were obtained for $Mn_{54}Al_{46}$ annealed at 400 ° C for 10 min

*Q. Zeng, I. Baker, J.B. Cui, Z.C. Yan, JMMM, 308 (2007) 214–226

K. Anand et al. / Journal of Alloys and Compounds 601 (2014) 234–237

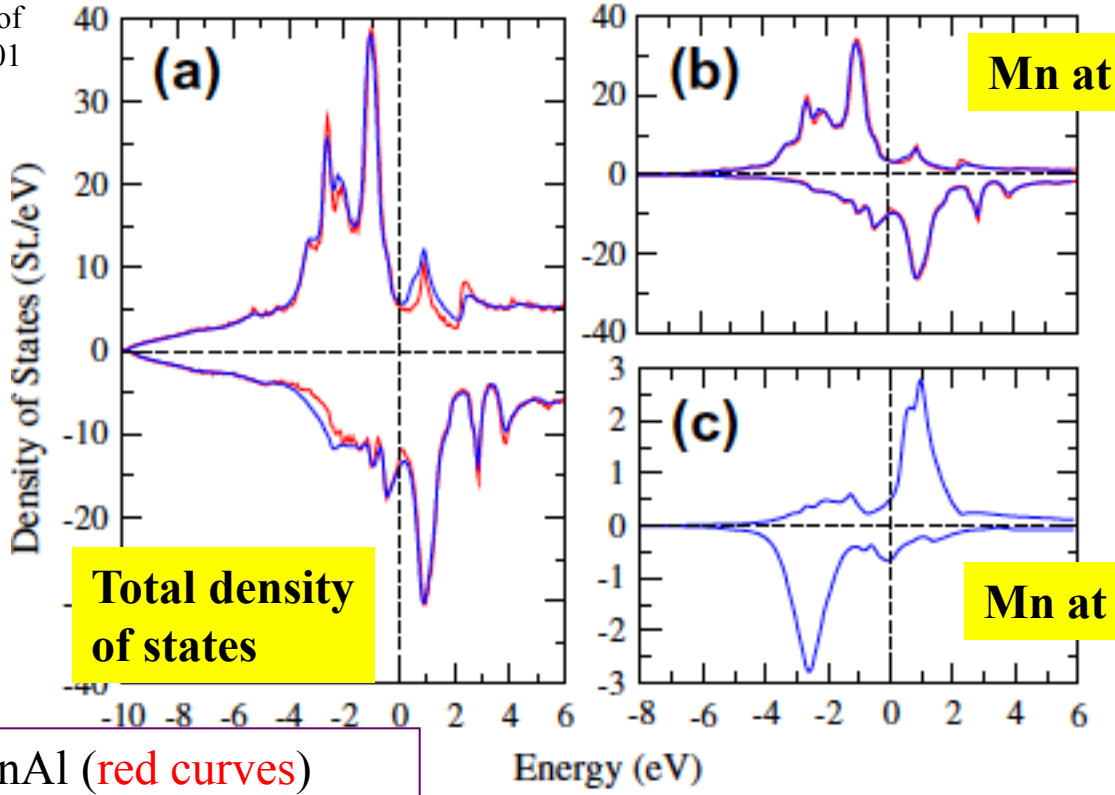

stoichiometric MnAl (red curves)
$Mn_{50+\delta}Al_{50-\delta}$; δ=4 (blue curves) .

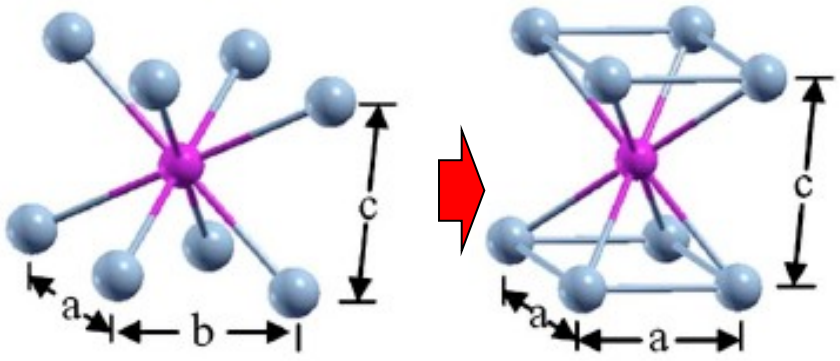

ε'-phase τ-phase-P4/mmm

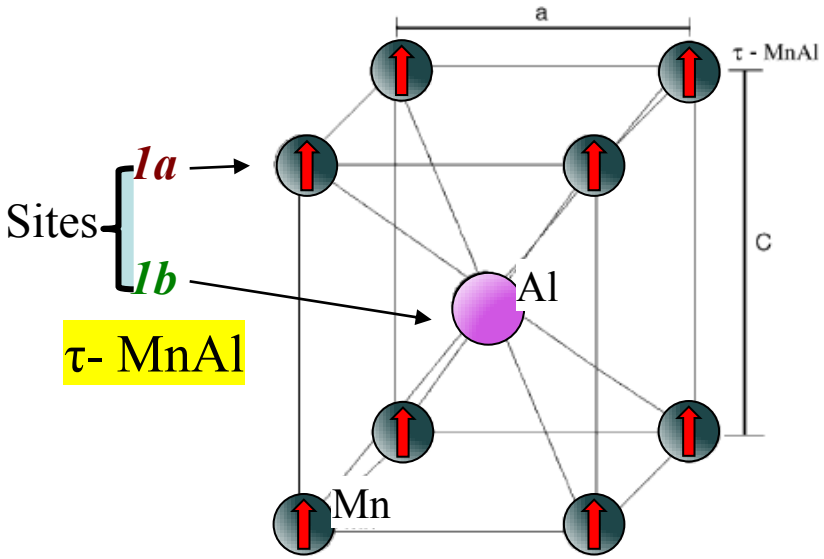

Our results

$Mn_{50}Al_{46}Ni_4$ and $Mn_{54}Al_{46}$

- Ingots were prepared by arc or induction melting
- Different heat treatment to stabilize the desired magnetic phase

Measurements

- Differential thermal analysis (DTA)
- XRD on Brüker D8 Advance diffractometer
- Thermomagnetic measurements up to 800 K

Electronic structure calculations

were performed in the framework of the Local Density Approximation (LDA) of the Density Functional Theory [31] using the SPRKKR method. The calculation method is based on the KKR-Green's function formalism that makes use of multiple scattering theories

DTA_$Mn_{50}Al_{46}Ni_4$ and $Mn_{54}Al_{46}$

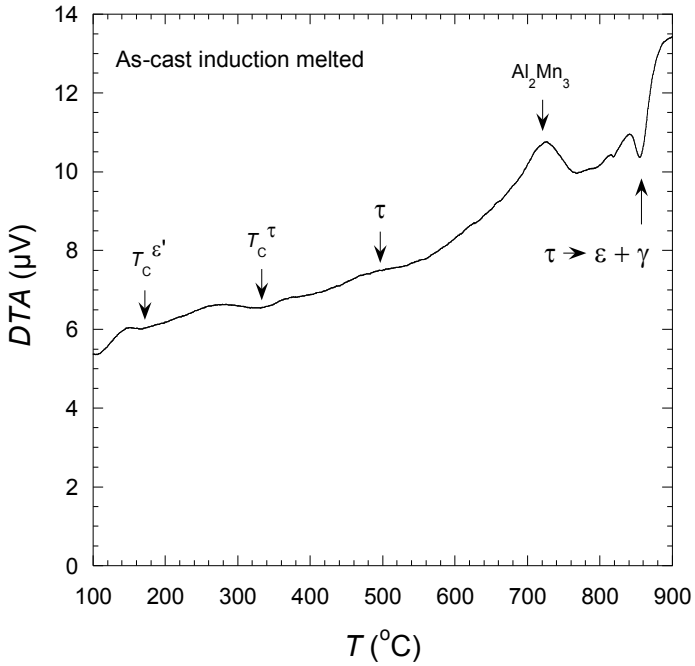

Fig. 1. DTA curve for the as-cast $Mn_{50}Al_{46}Ni_4$ alloy.

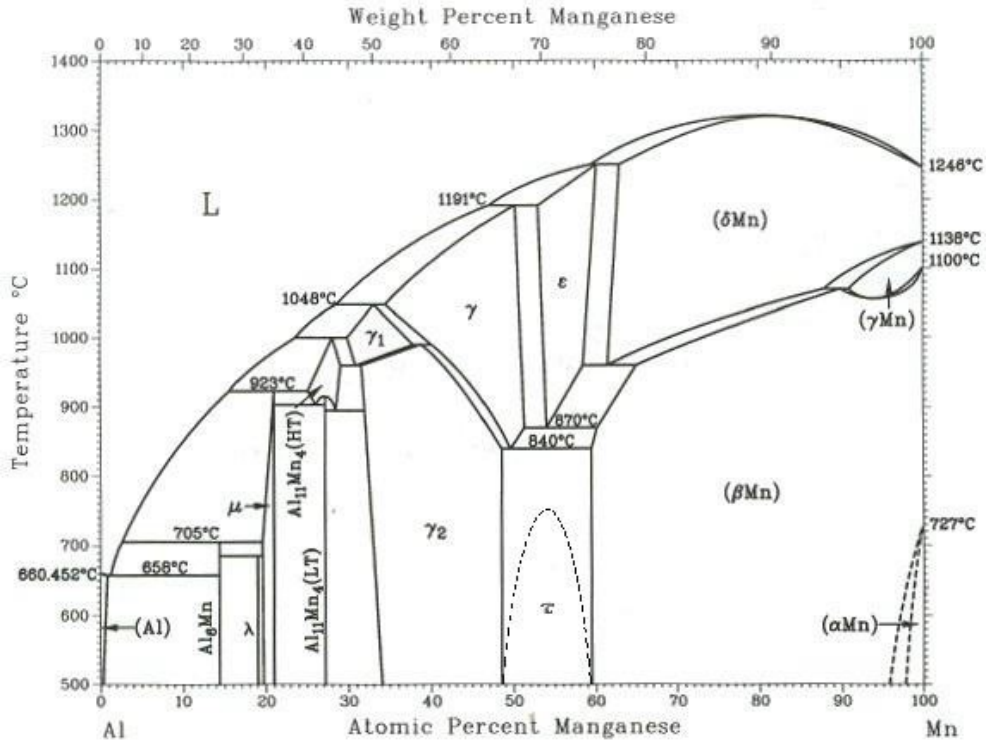

XRD

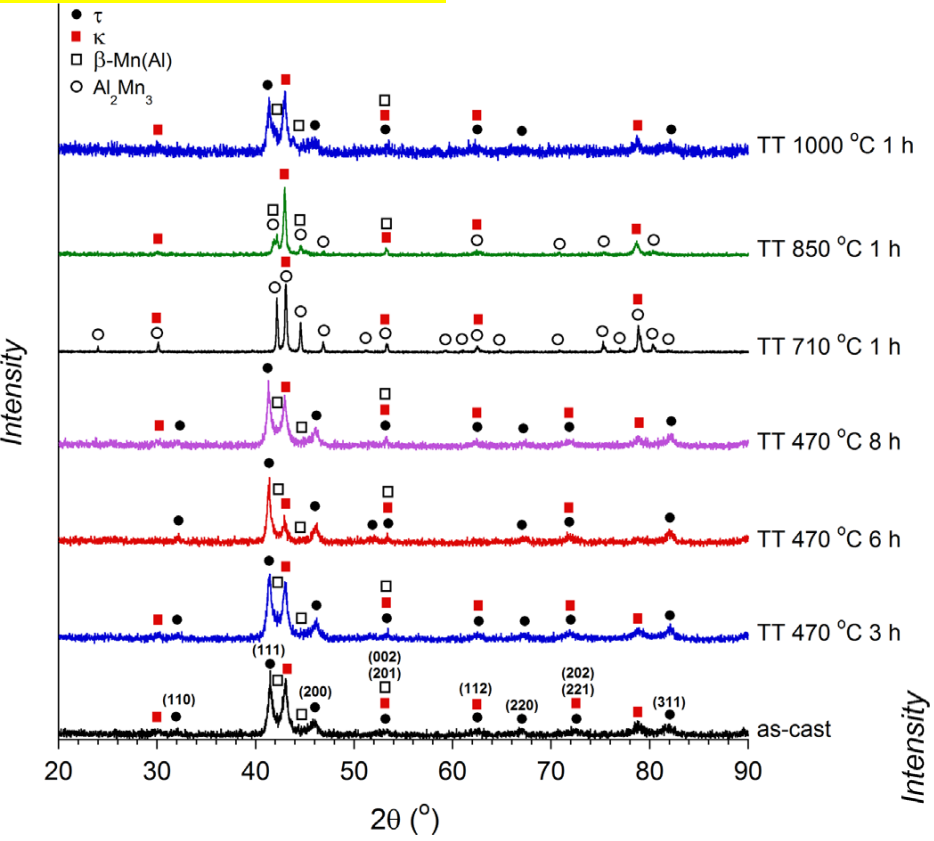

$Mn_{50}Al_{46}M_4$ – different heat treatments

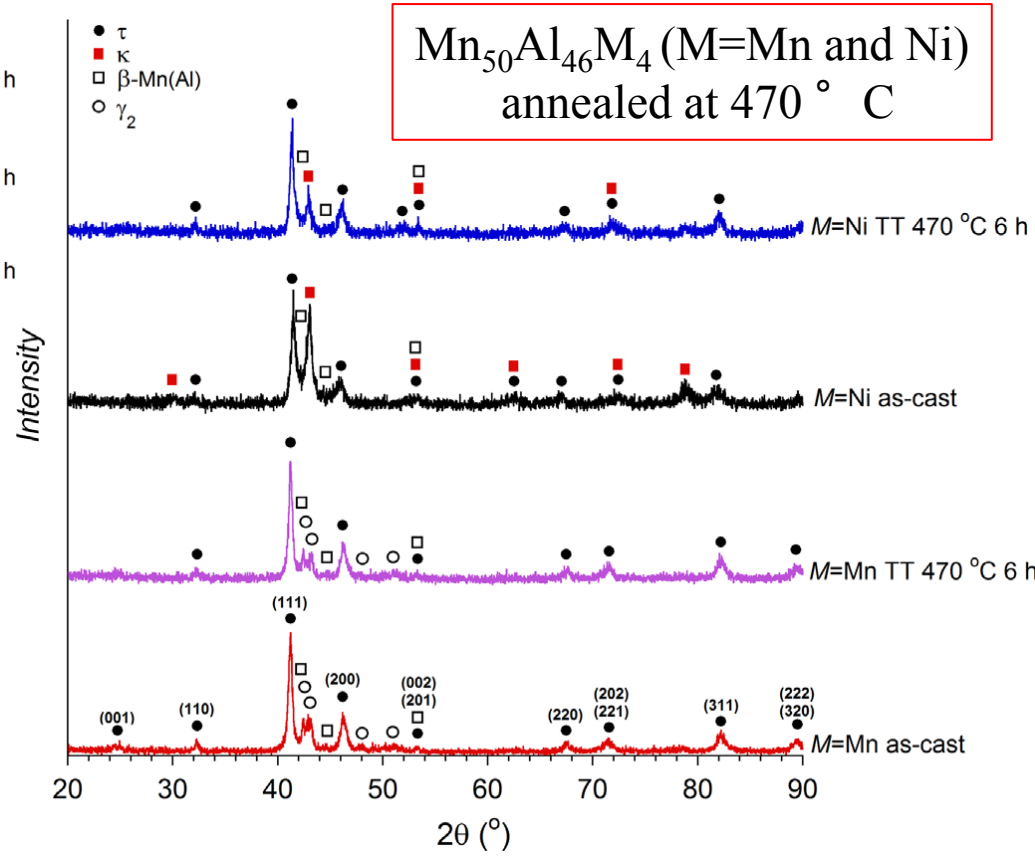

$Mn_{50}Al_{46}M_4$ (M=Mn and Ni) annealed at 470 ° C

S. Mican, D. Benea, R. Hirian, R. Gavrea, O. Isnard, V. Pop, M. Coldea /JMMM 401 (2016) 841–847

Some XRD results

Sample	a (Å)	c (Å)	c_τ (wt%) ± 2%	$c_{\gamma 2}$ (wt%) ± 2%	c_β (wt%) ± 2%	c_κ (wt%) ± 2%
$Mn_{54}Al_{46}$ as-cast	3.93	3.57	68	25	7	–
$Mn_{54}Al_{46}$ + 470 °C 6 h	3.93	3.57	76	20	4	–
$Mn_{50}Al_{46}Ni_4$ as-cast	3.96	3.47	50	–	5	45
$Mn_{50}Al_{46}Ni_4$ + 470 °C 6 h	3.94	3.52	74	–	6	20

τ phase

Band structure (SPRKKR) calculations: $Mn_{54}Al_{46}$ and $Mn_{50}Al_{46}Ni_4$ in the AFM configuration.

Sample	Atom	m_{spin} (μ_B)	m_{orbit} (μ_B)
$Mn_{54}Al_{46}$	Al^{2e}	−0.08	0
	Mn^{2e}	−3.22	−0.01
	$Mn^{1a,1c}$	2.33	0.04
	Total (μ_B/f.u.)	**1.00**	**0.02**
$(Mn_{46}\ Ni_4)^{1a,1c}(Al_{46}Mn_4)^{2e}$	$Mn^{1a,1c}$	2.27	0.04
	$Ni^{1a,1c}$	−0.09	−0.01
	Al^{2e}	−0.08	0
	Mn^{2e}	−3.21	−0.02
	Total (μ_B/f.u.)	**0.88**	**0.02**

Thermomagnetic studies

$Mn_{50}Al_{46}Ni_4$ and $Mn_{54}Al_{46}$

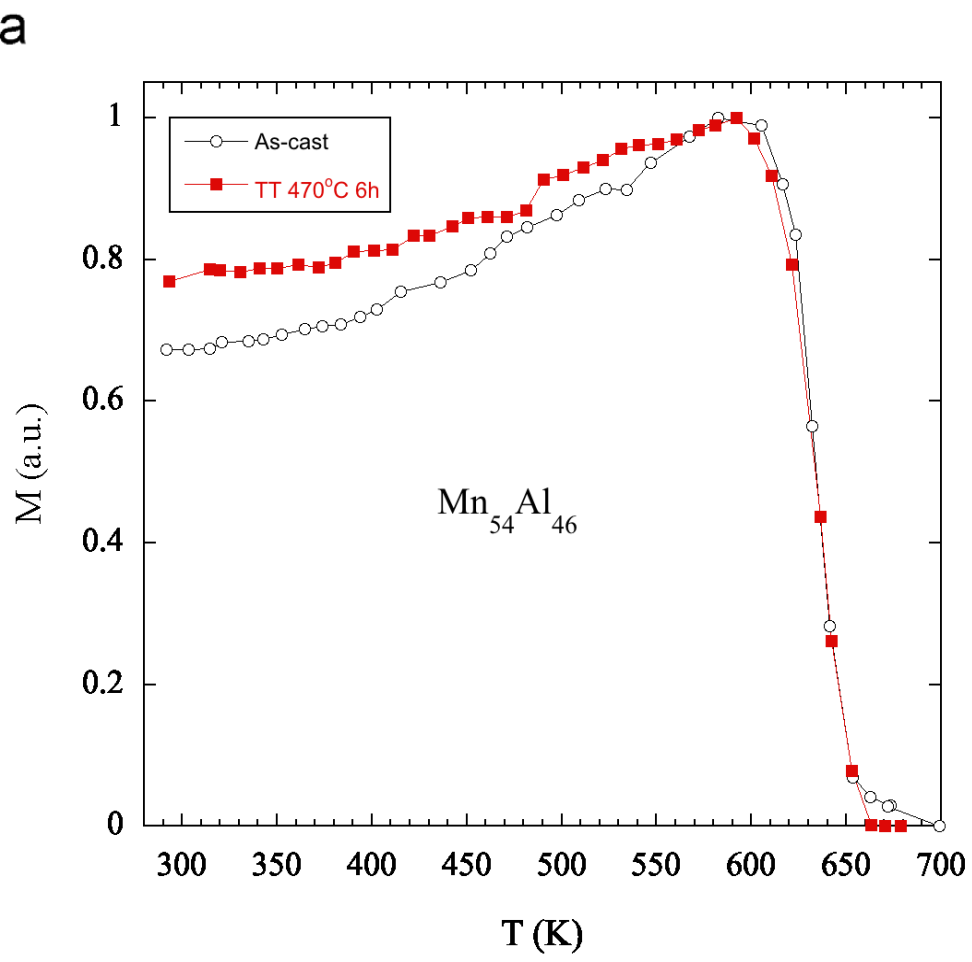

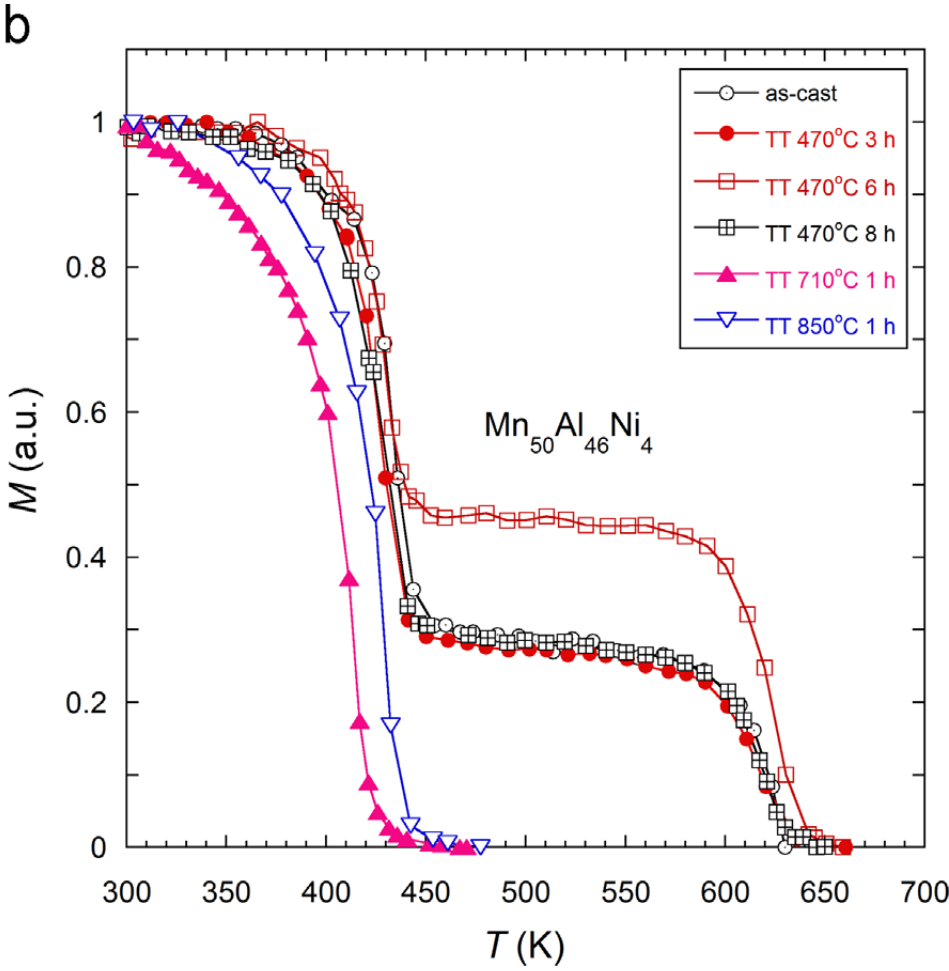

S. Mican, D. Benea, R. Hirian, R. Gavrea, O. Isnard, V. Pop, M. Coldea /JMMM 401 (2016) 841–847

Magnetic behavior

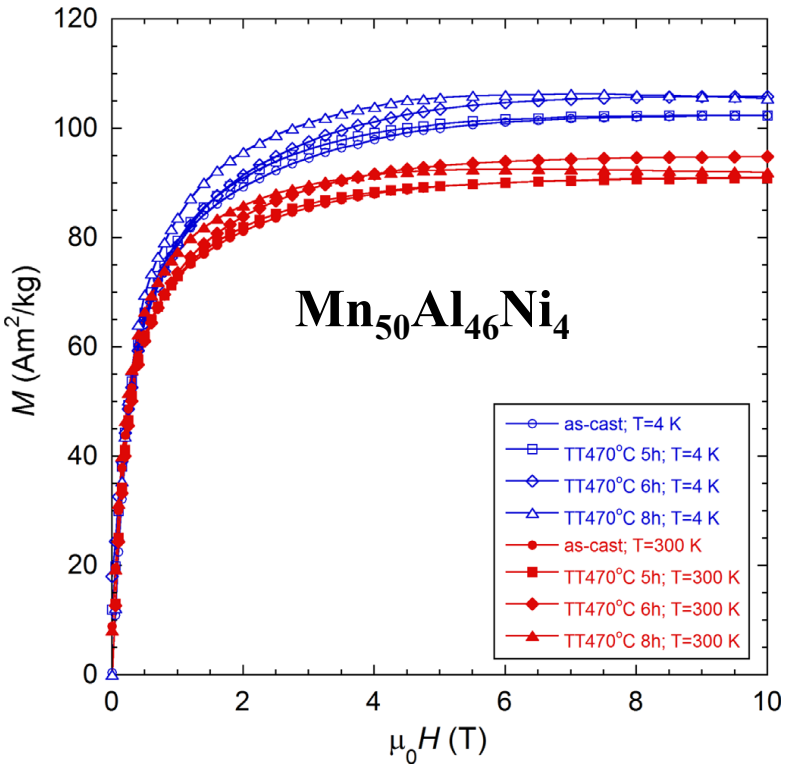

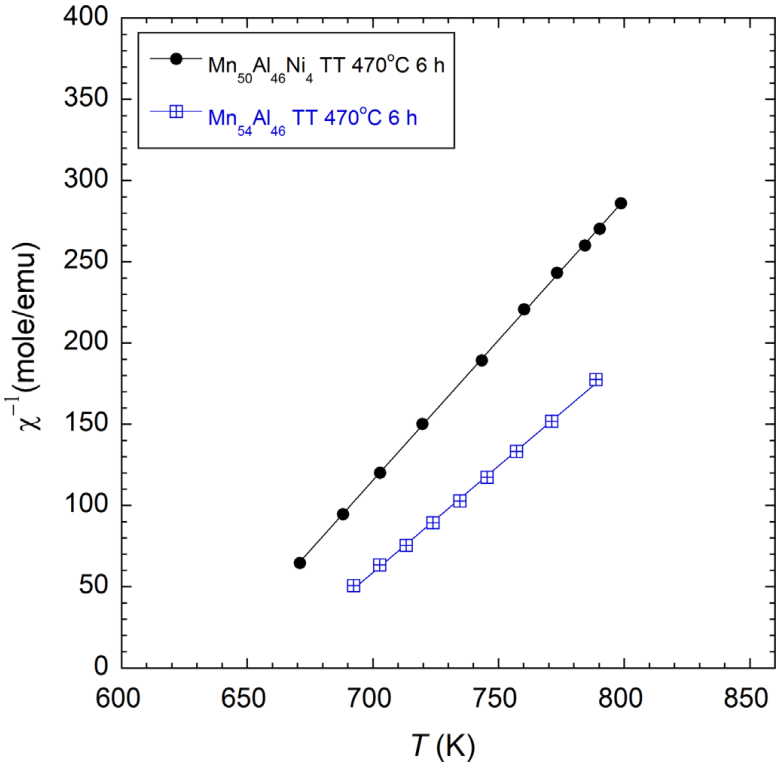

Table 3. The magnetic moments in the ordered (m) and paramagnetic state (μ_{eff}), the ferromagnetic (T_c) and paramagnetic (θ) Curie temperatures for the $Mn_{54}Al_{46}$ and $Mn_{50}Al_{46}Ni_4$ alloys annealed at 470°C for 6h.

Sample	m_{tot} (μ_B/f.u.)	m_{Mn} (μ_B/Mn atom)	T_c (K)	μ_{eff} (μ_B/f.u)	θ (K)	μ_{eff}^{τ} (μ_B/Mn atom)	$\mu_{eff}^{\gamma 2}$ (μ_B/Mn atom)	μ_{eff}^{β} (μ_B/Mn atom) [43]	μ_{eff}^{κ} (μ_B/Mn atom)
$Mn_{54}Al_{46}$	1.11	2.41	645	2.47	655	3.26	3.94	1.70	-
$Mn_{50}Al_{46}Ni_4$	0.92	2.19	634	2.15	633	3.03	-	1.70	3.37

S. Mican, D. Benea, R. Hirian, R. Gavrea, O. Isnard, V. Pop, M. Coldea /JMMM 401 (2016) 841–847

Outline

- Introduction
- Mn-Al and Mn-Bi magnetic phase
- **Nanocomposites magnets=Spring magnets**
- Conclusions

magnetit magnet (1750)

10 cm

ferrite magnet (1940)

rare earth based magnet (1980)

exchange-spring magnets (20??)

All this magnets have the same energy !

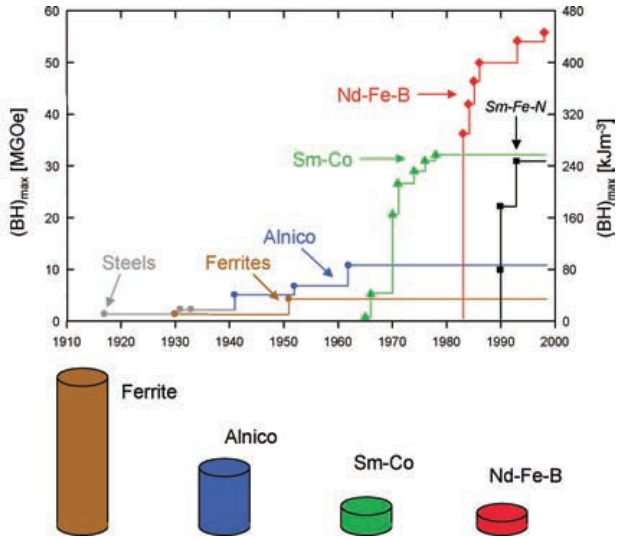

$$\vec{B} = \mu_0 \vec{H} + \mu_0 \vec{M}$$

$$\mu_0 \vec{H} + \vec{J}$$

$$(BH)_{\max} = \frac{J_r^2}{4\mu_0}$$

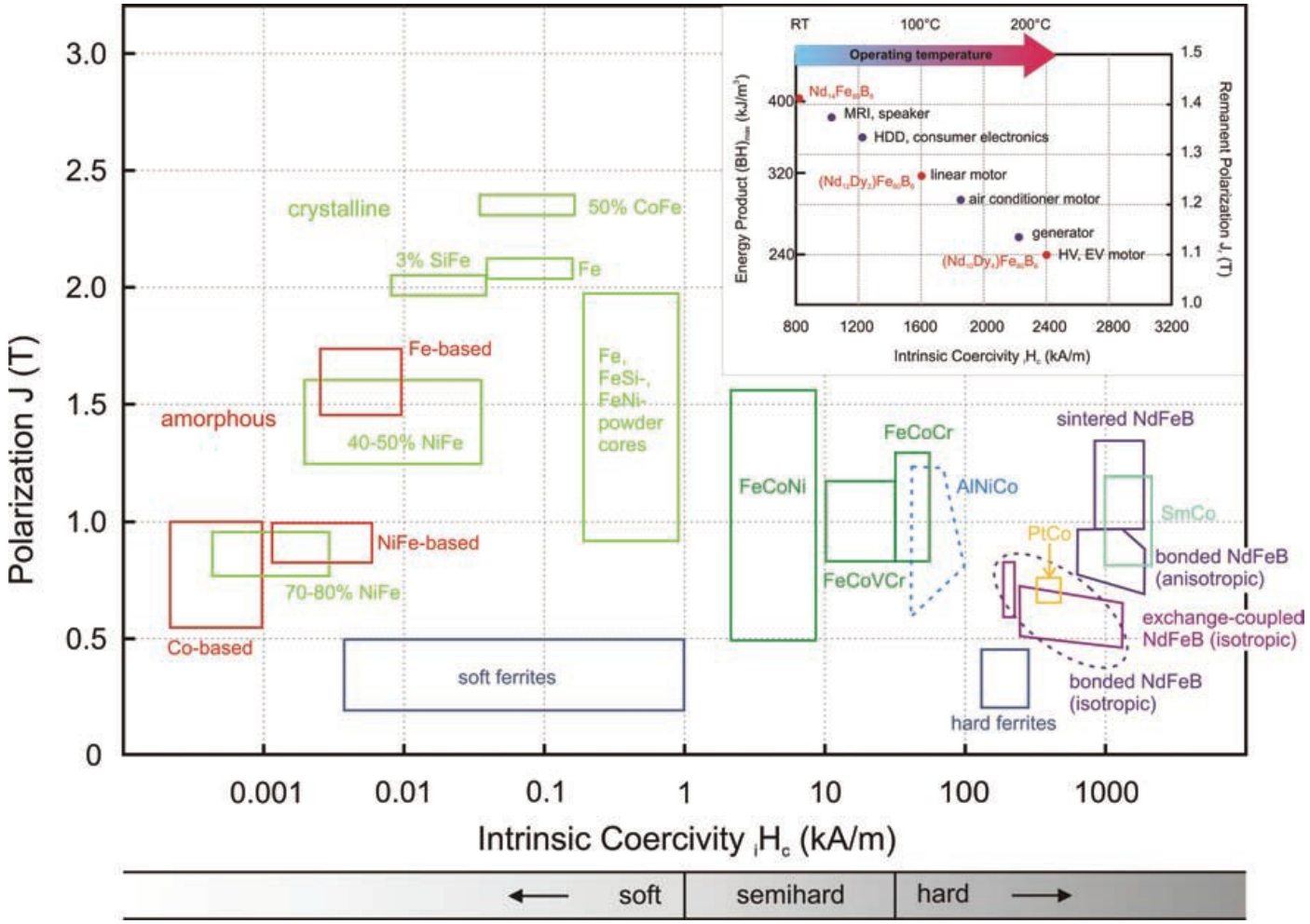

*O. Gutfleisch , M. A. Willard, E. Brück, C.a H. Chen, S. G. Sankar, and J. P. Liu, Adv. Mater. 2011, 23, 821–842)

Theoretical predictions:

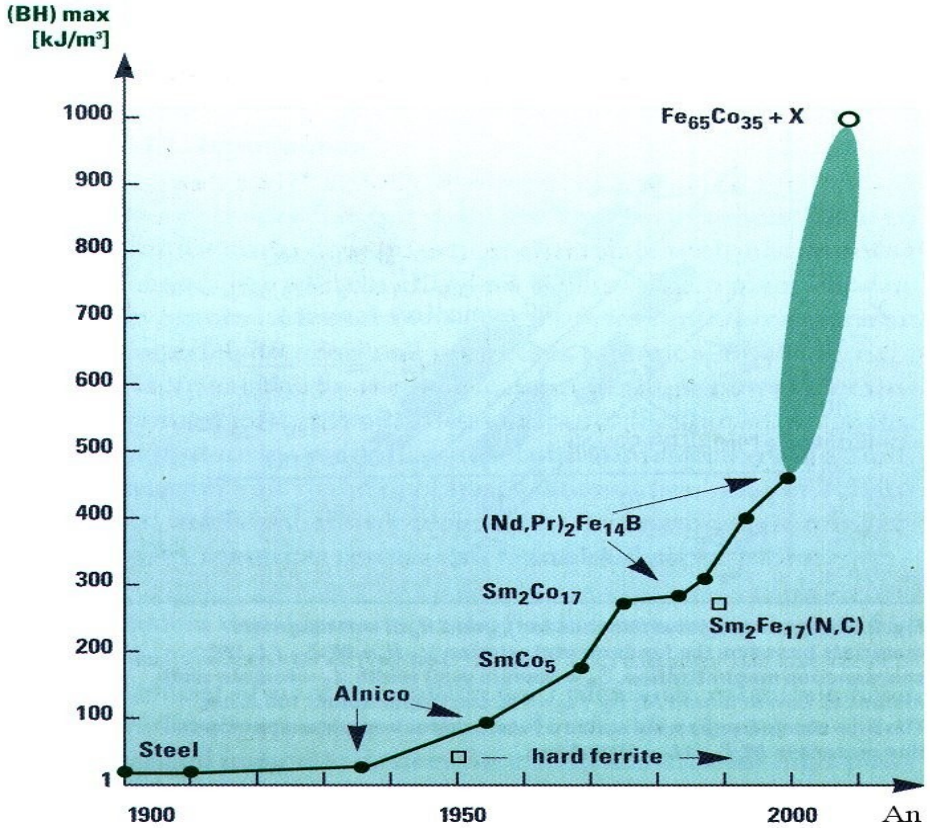

Best magnets on the market: (BH)max ≈ 500 kJ/m3

$(BH)_{max}$ = 1090 kJ/m³ for nanostructured multilayers $Sm_2Fe_{17}N_3/Fe_{65}Co_{35}$

R. Skomski, J. Appl. Phys. 76 (1994) 7059

Kronmuller & Coey *Magnetic Materials*, in *European White book on Fundamentel Research in Materials Science* Max Planck Inst. Metallforschung, Stuttgart, 2001, 92-96

Experimental realisations: ??????????

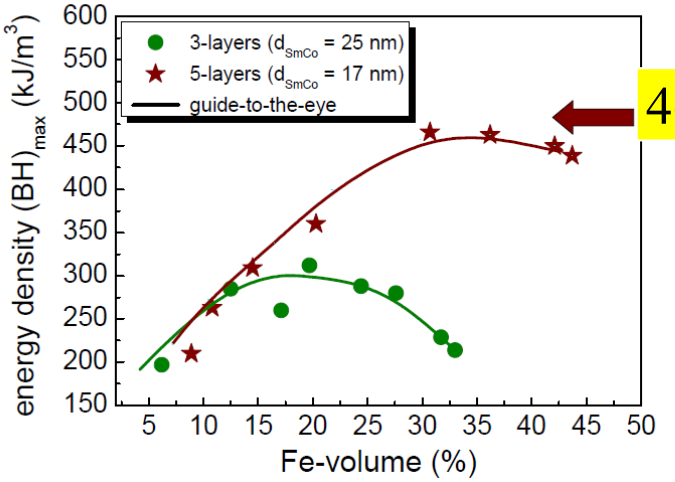

460 kJ/m³

V. Neu , S. Sawatzki , M.Kopte , Ch. Mickel , L. Schultz, IEEE TRANS. MAGN., 48 (2012) 3599,

Structure
Microstructure → **Soft-hard exchange hardness**

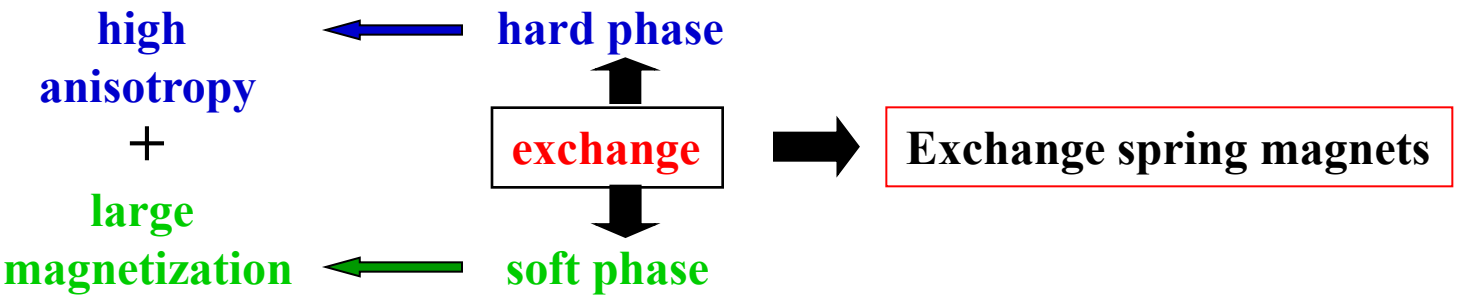

$$D_{cr} \approx 2\delta_h$$

$$\delta_h = \pi\sqrt{A_h / K_h}$$

D_{cr} = **soft phase critical dimension**
δ_h = width of domain wall in the hard phase
A_h and K_h are the exchange and anisotropy constants

Our researches

- hard magnetic phases of $SmCo_5$, $SmCo_3Cu_2$, $R_2Fe_{14}B$
- soft magnetic phases of α-Fe, Fe-Co (~20 or 10 wt%)

Magnetic Hard/Soft nanocomposites – Spring magnets

($SmCo_5$, $SmCo_3Cu_2$, $R_2Fe_{14}B$)+x% (α-Fe or $Fe_{65}Co_{35}$

- composition, x= 10 or 22 wt % Fe
- milling time
- conventional annealing/short time annealing

Material preparation

- milling of the powders in a high energy planetary mill
- heat treatments (temperatures and duration)

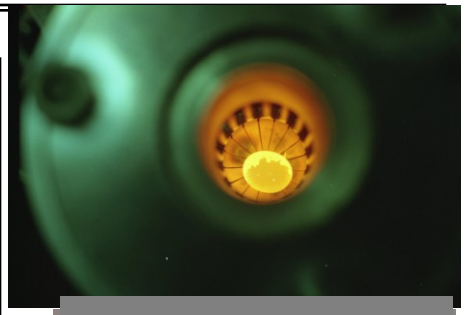

Fritsch Pulverisette 4

Starting materials :

- **hard magnetic phases**
  ingots – prepared by melting
- **Fe NC 100.24 powder (Höganäs), (< 40 μm) and**
- **$Fe_{65}Co_{35}$ obtained by melting**

Mechanical milling experiments:

- **premilling of hard and soft magnetic ingots**
- **hard magnetic + α-Fe (or $Fe_{65}Co_{35}$)** mixed powders – milled in Ar for **1.5 – 12** h

Annealing:

- **conventional annealing:** **in vacuum/450-650 ° C for 0.5 up to 10 h.**
- **short time annealing:** **in argon/700, 750 or 800 ° C for 0.5 to 3 min.**

Material characterisation

- X-rays diffraction (XRD)
- DSC measurements
- Electron microscopy (SEM and TEM)
  - morphology
  - chemical composition checked by EDX
- Magnetic measurements
- Mössbauer spectroscopy
- Atom probe tomography (APT)

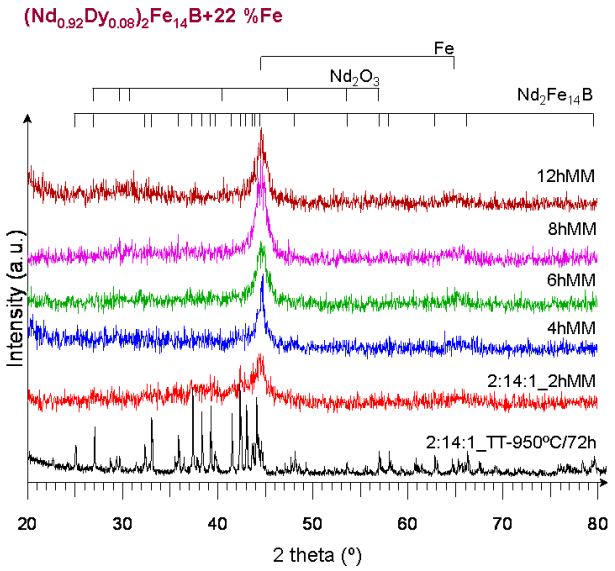
$(Nd_{0.92}Dy_{0.08})_2Fe_{14}B$+22 %Fe
Fe
Nd_2O_3
$Nd_2Fe_{14}B$
12hMM
8hMM
6hMM
4hMM
2:14:1_2hMM
2:14:1_TT-950ºC/72h
Intensity (a.u.)
20
30
40
50
60
70
80
2 theta (º)

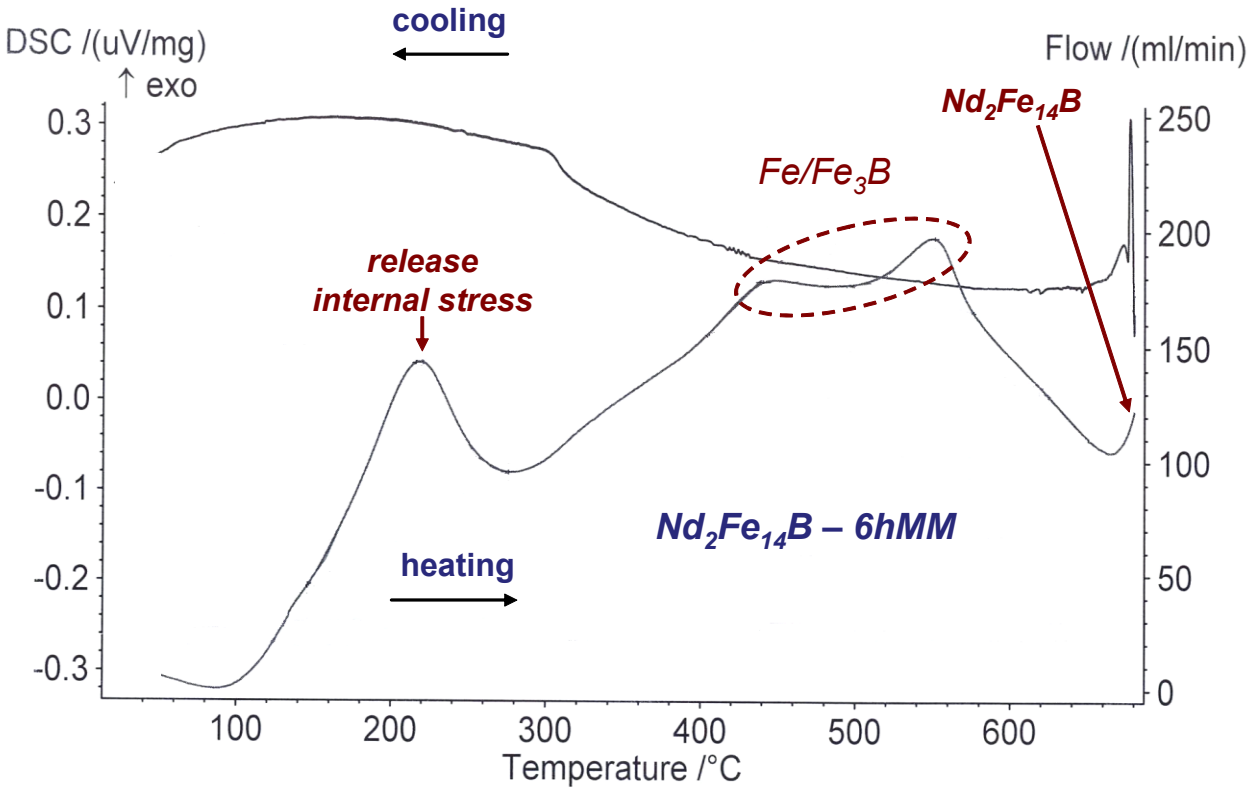
cooling
DSC /(uV/mg)
↑ exo
Flow /(ml/min)
$Nd_2Fe_{14}B$
Fe/Fe_3B
release
internal stress
$Nd_2Fe_{14}B$ – 6hMM
heating
0.3
0.2
0.1
0.0
-0.1
-0.2
-0.3
250
200
150
100
50
0
100
200
300
400
500
600
Temperature /°C

Short time annealing

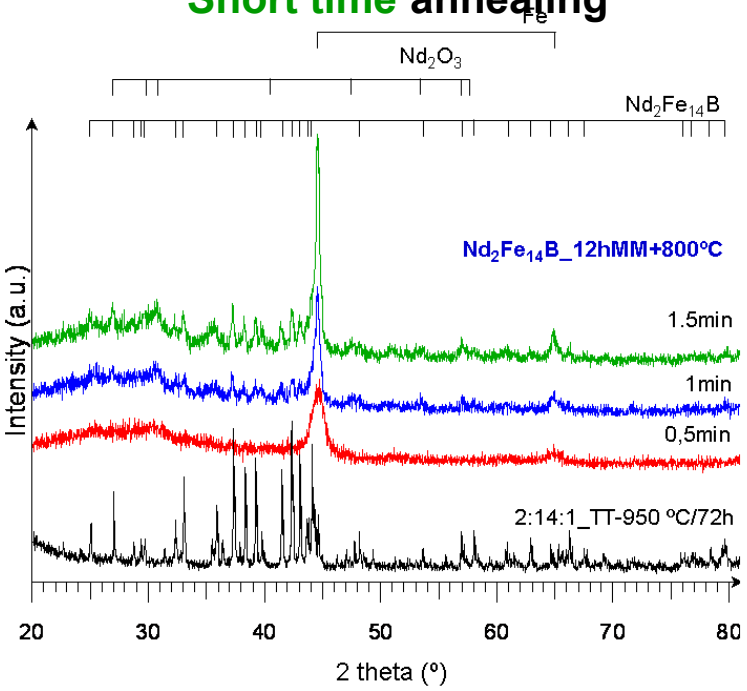

Classical annealing

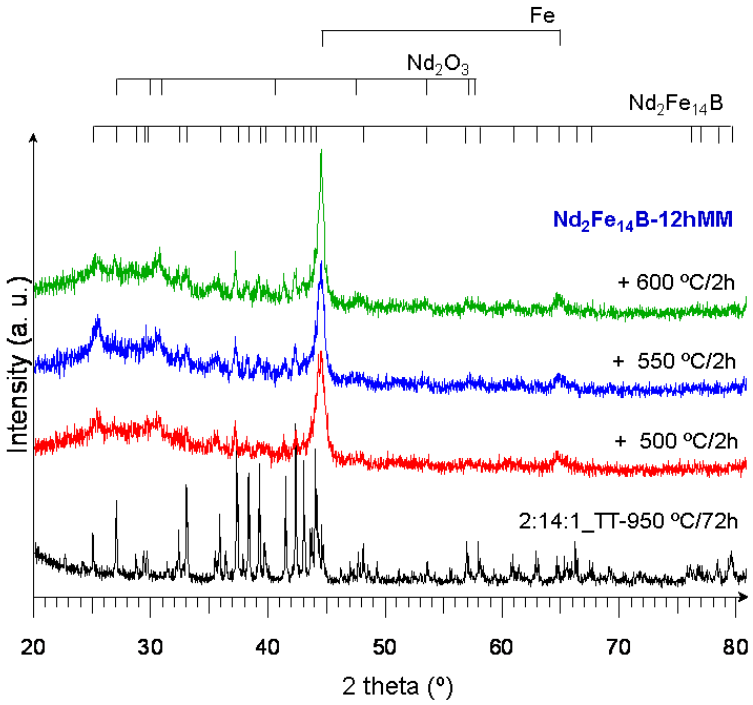

Microstructure; $Nd_2Fe_{14}B$+10 wt% Fe

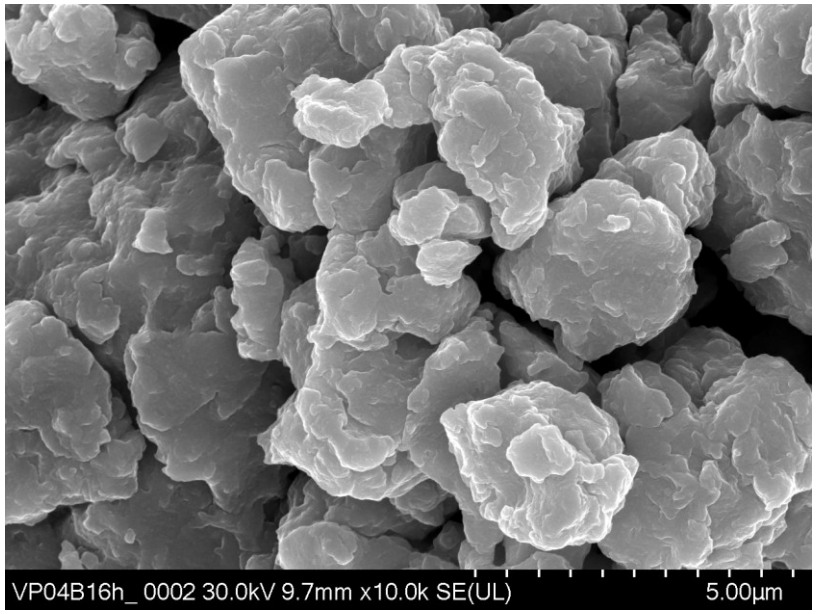

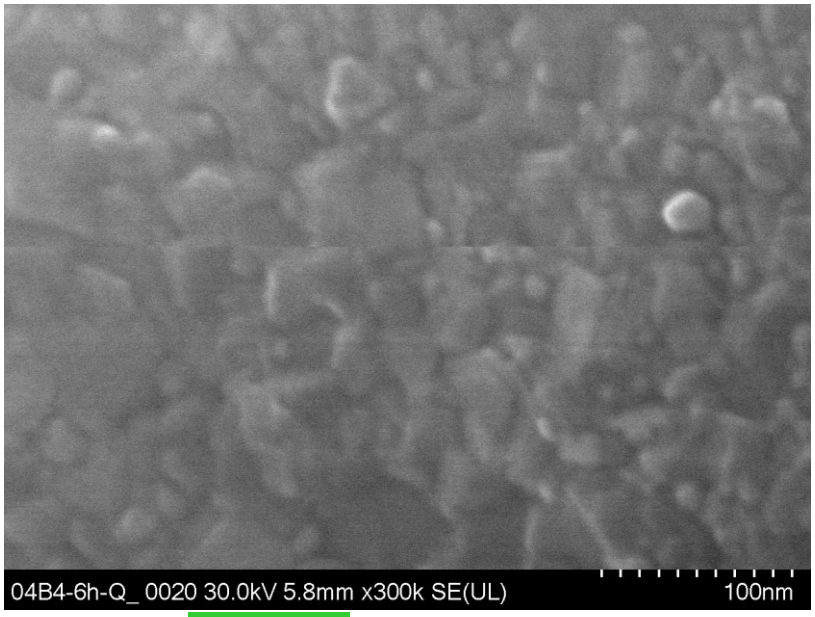

TEM

$SmCo_5$ + 20% α-Fe
6h MM+450 °C/0.5h

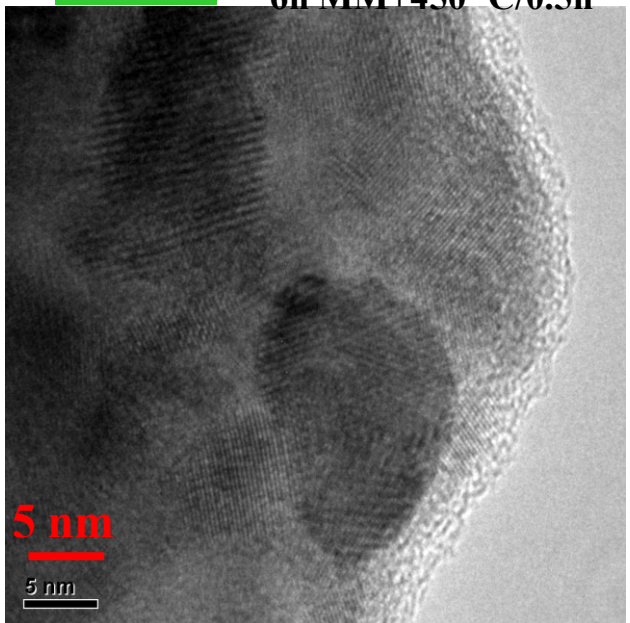

From XRD measurements

$$D = \frac{K \cdot \lambda}{\beta \cdot \cos\theta}; \quad \beta \equiv \beta_{1/2} \Rightarrow K = 0.9$$

For 6 h or more MM sample D < 30 nm

Microstructure/ composition

$SmCo_5$+20 wt% Fe; Atomic-Scale Investigation

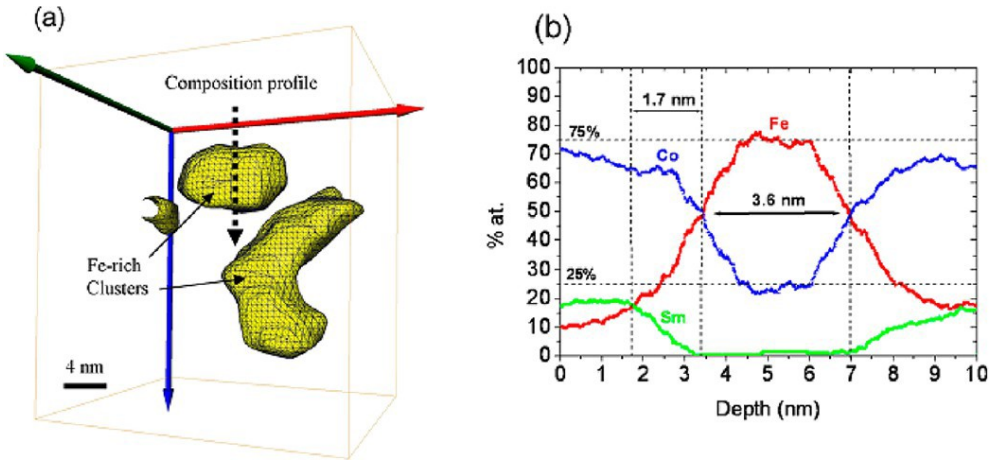

R. Lardé, J-M. Le Breton, A. Maître, D. Ledue, O. Isnard, V. Pop and I. Chicinaş, J. Phys. Chem., 117 (2013) 7801

$Nd_2Fe_{14}B$+10 wt% Fe

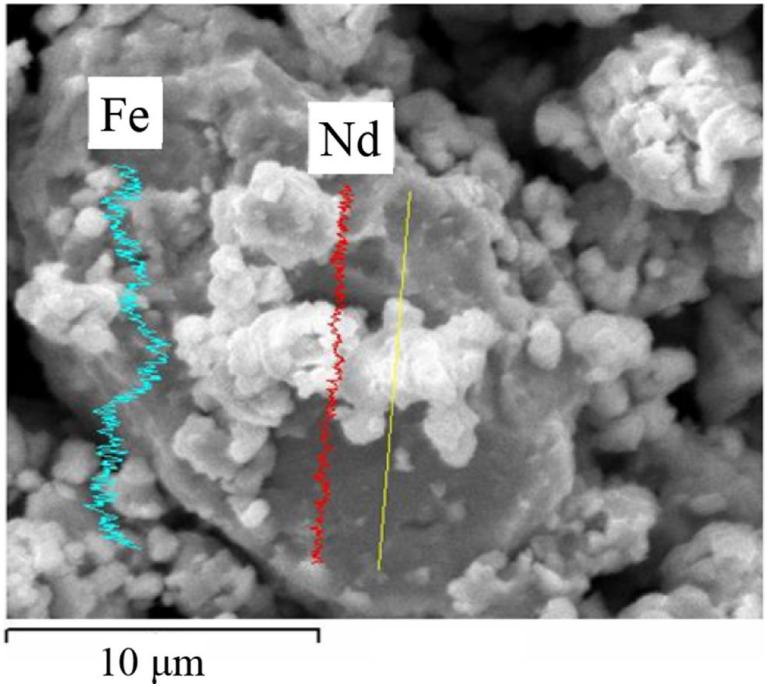

S. Gutoiu, O. Isnard. I. Chicinas, F. Popa, A. Takacs ,V. Pop / JALCOM 646 (2015) 859

Mossbauer studies/interphase diffusion

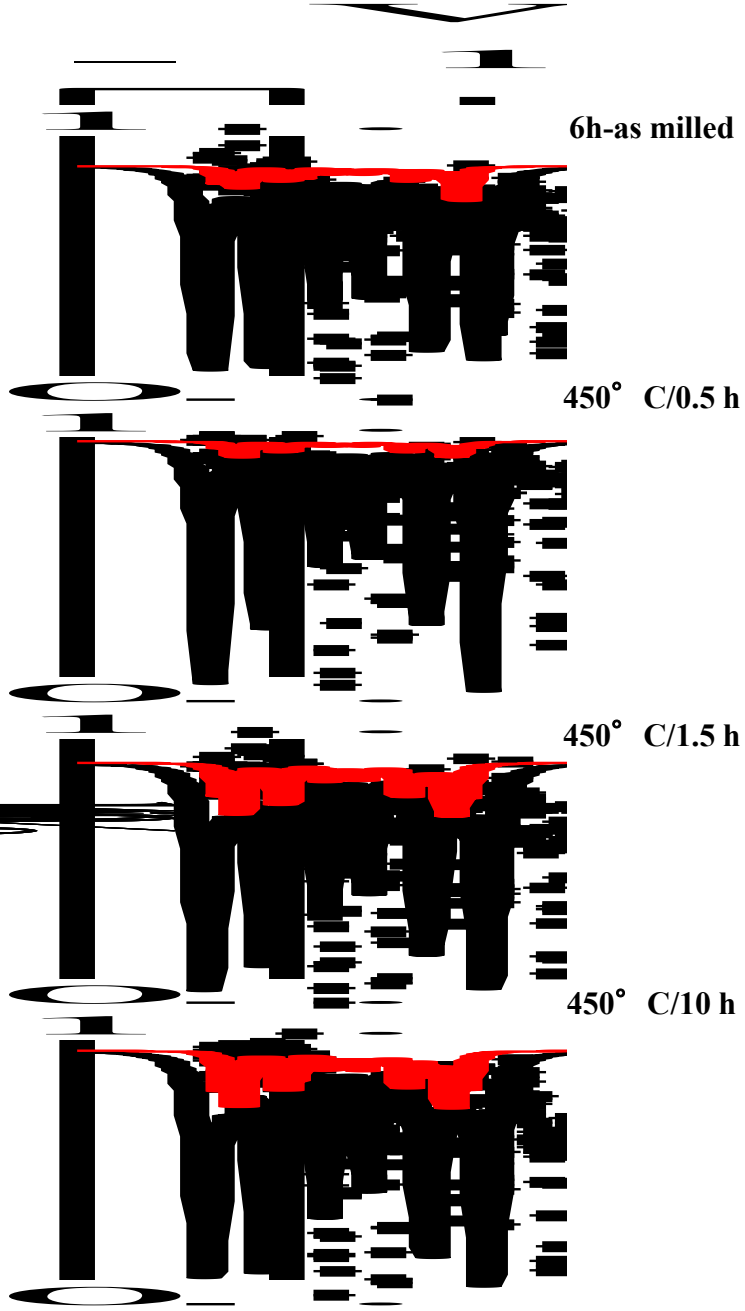

$SmCo_5$+20 wt% Fe

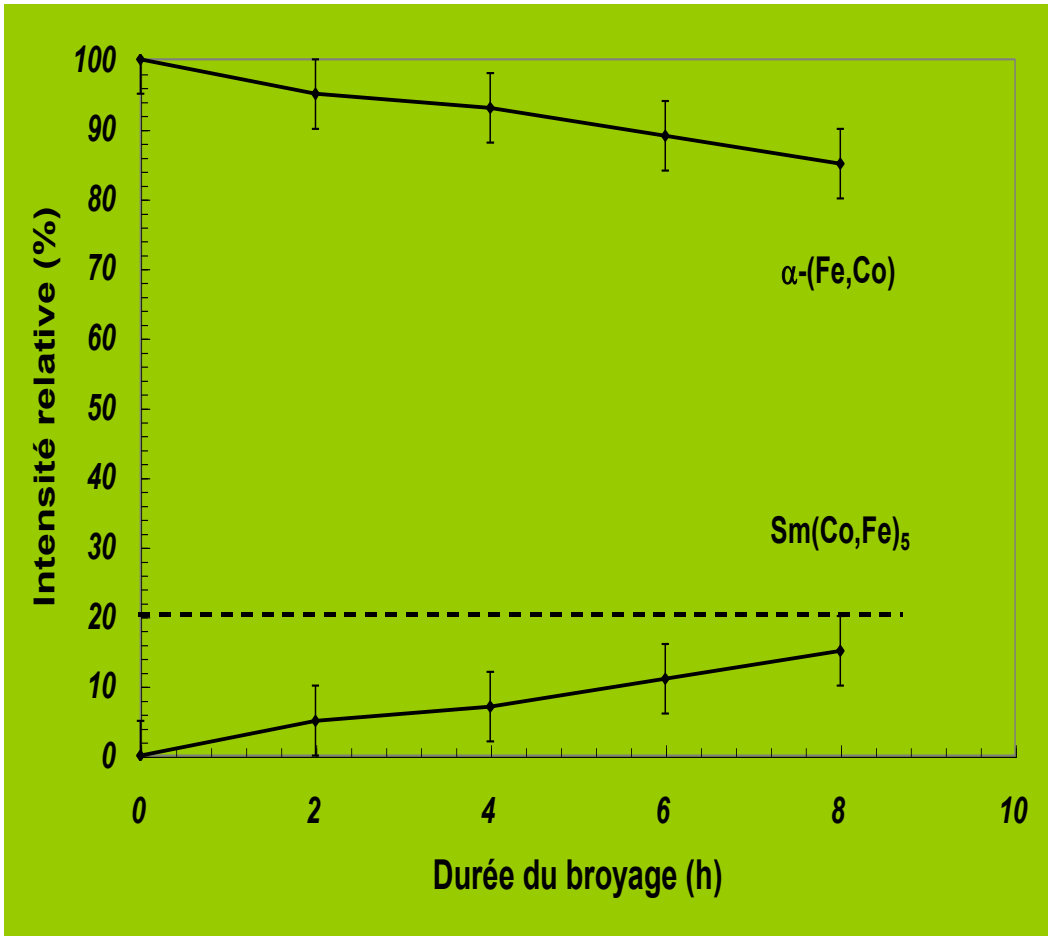

high anisotropy + large magnetization

hard phase

exchange

soft phase

Exchange spring magnets

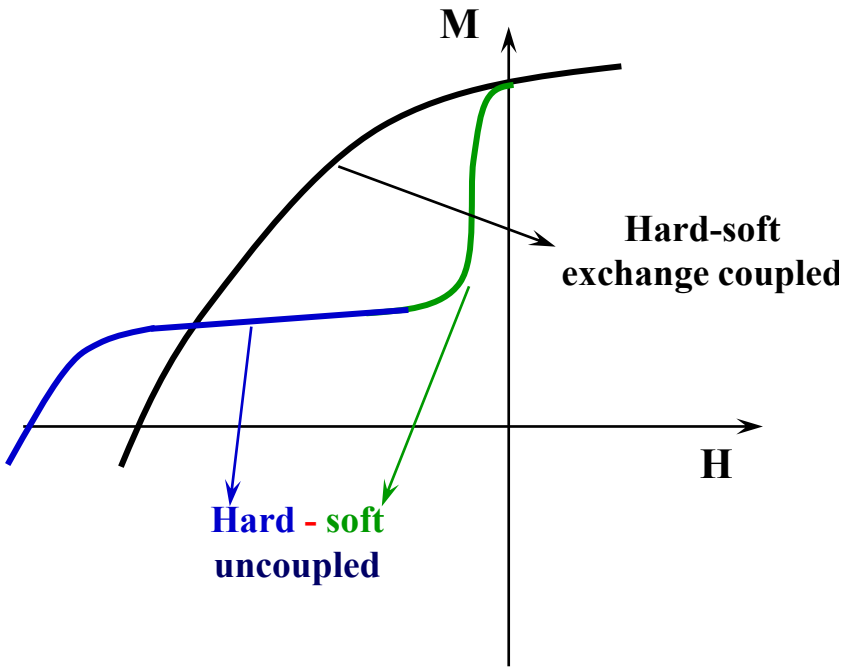

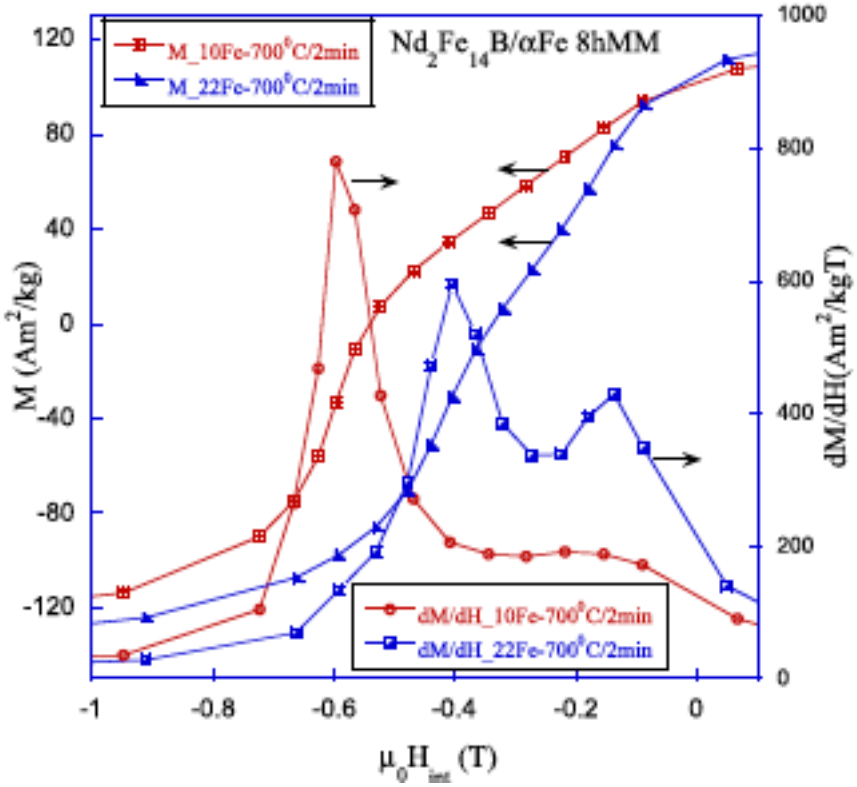

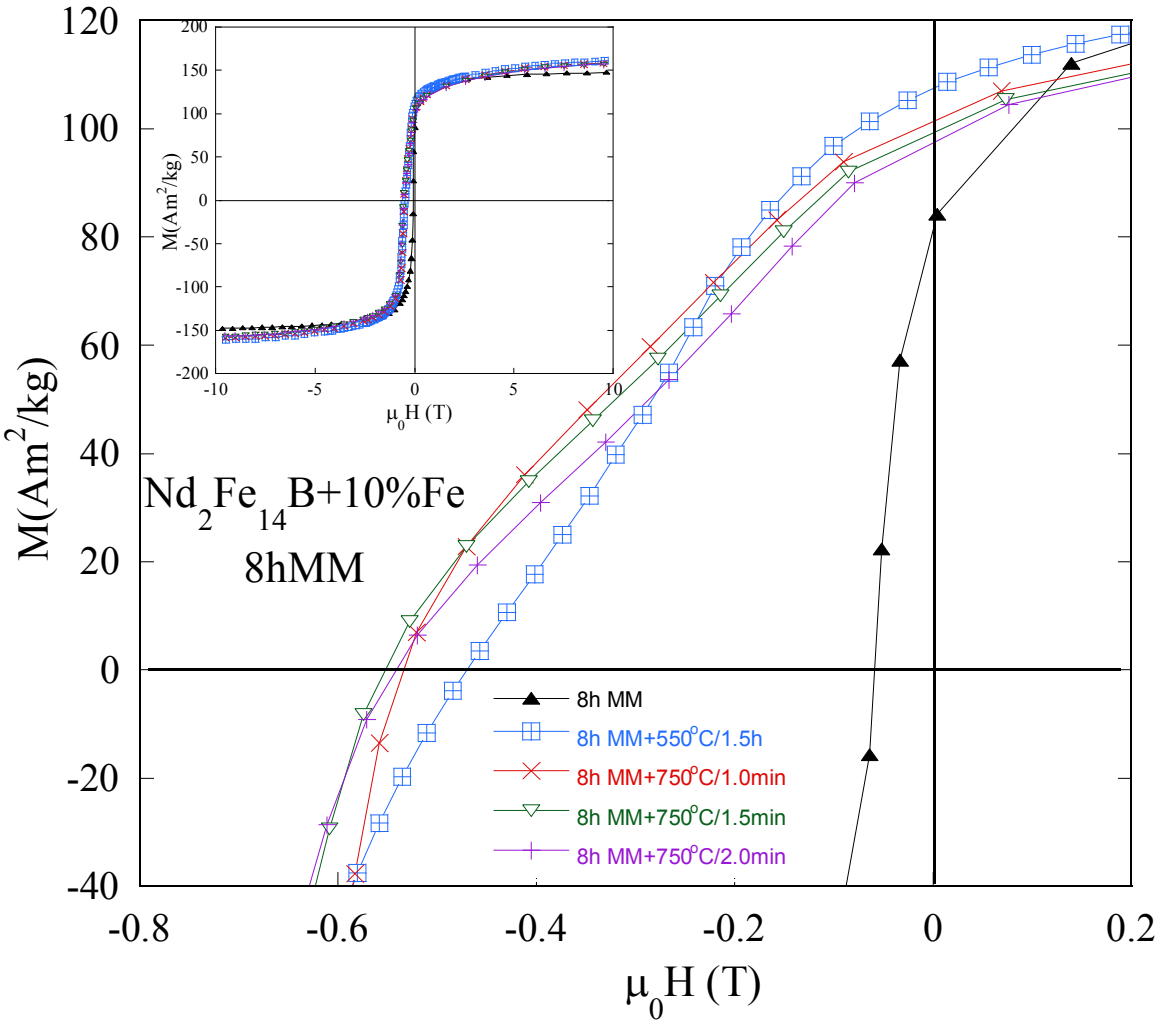

$Nd_2Fe_{14}B$ + 10 % α-Fe; 8h MM

Classical annealing ⟷ **Short time annealing**

H_c- evident increasing

M_r- small decreasing

The influence of the type of hard magnetic phase

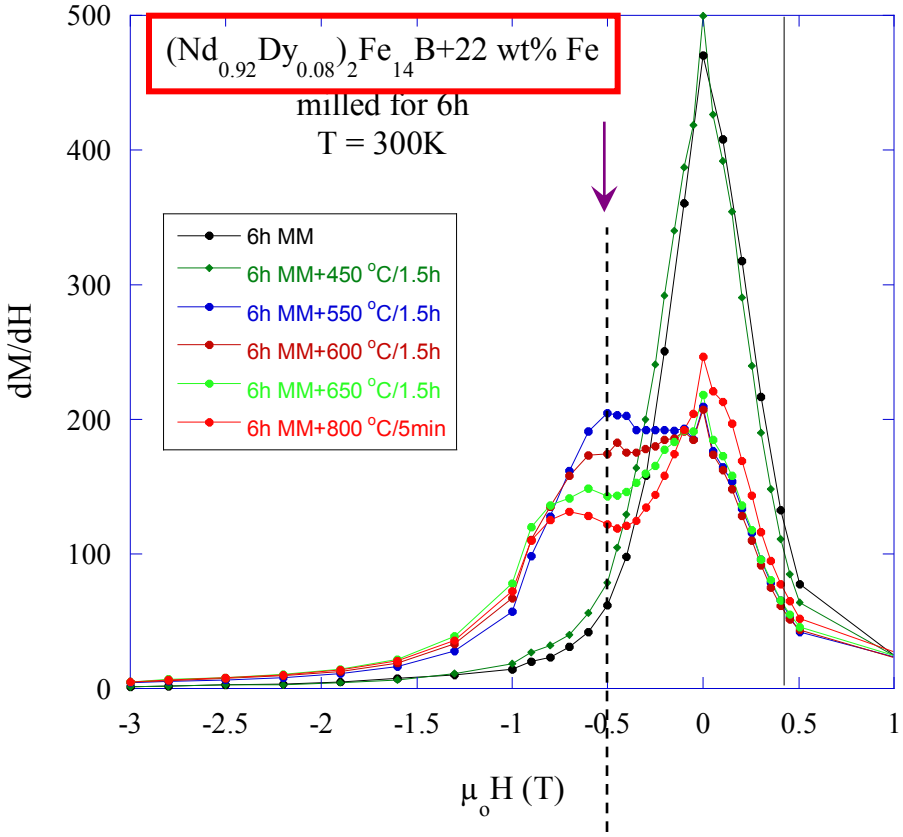

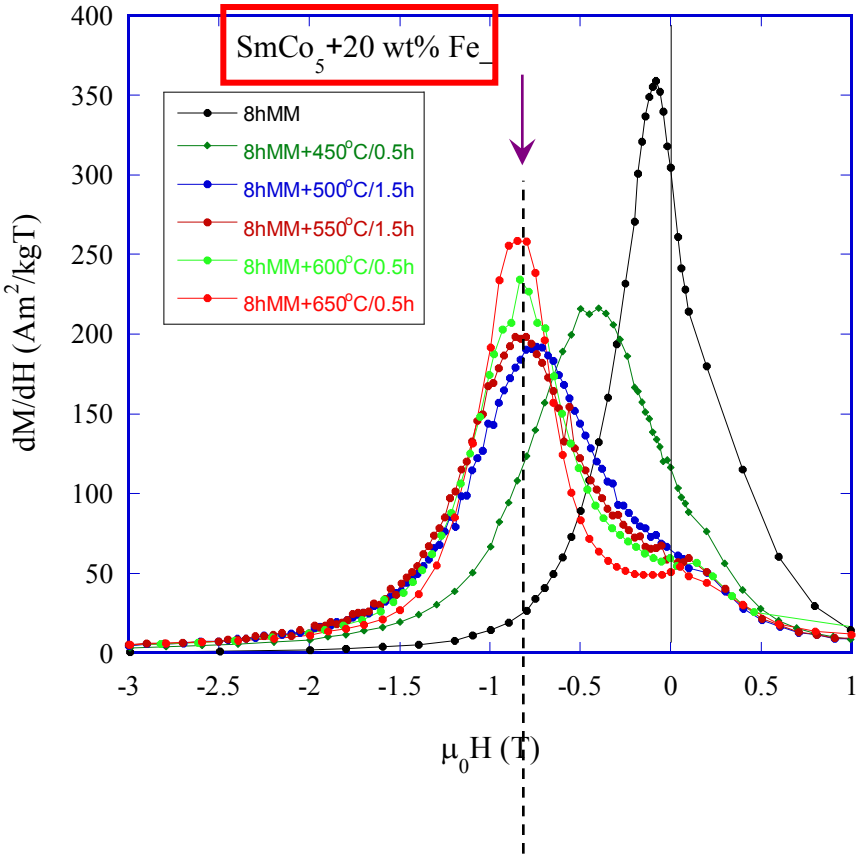

$R_2Fe_{14}B/Fe$

Lower coercivity
Two peaks,
pour hard/soft magnetic coupling

$SmCo_5/Fe$

Higher coercivity
One peak,
good hard/soft magnetic coupling

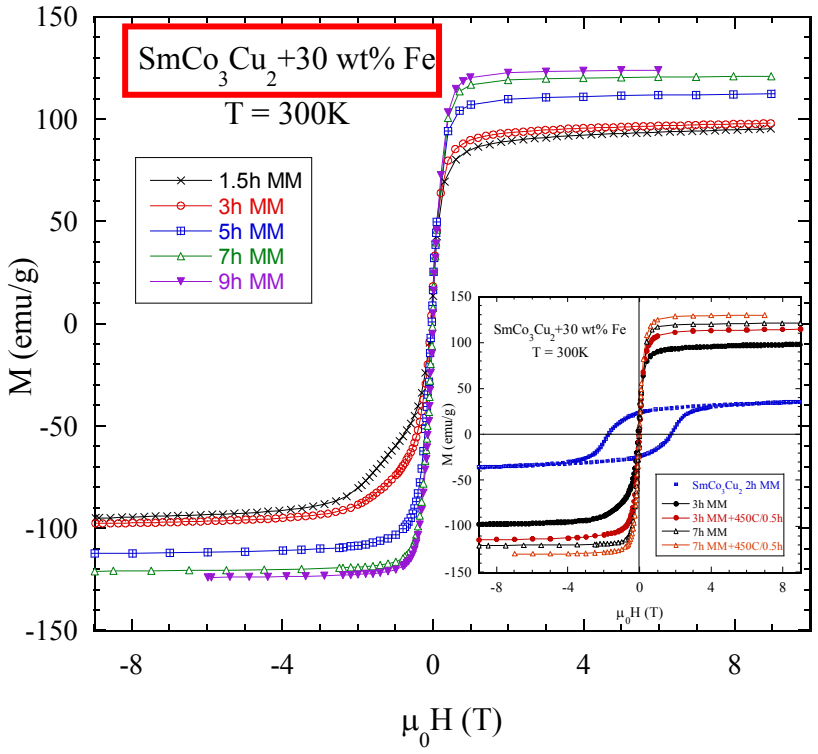

the importance of the
intrinsic anisotropy*

*D. Givord, O. Isnard,, V. Pop, I. Chicinas, JMMM 316 (2007)

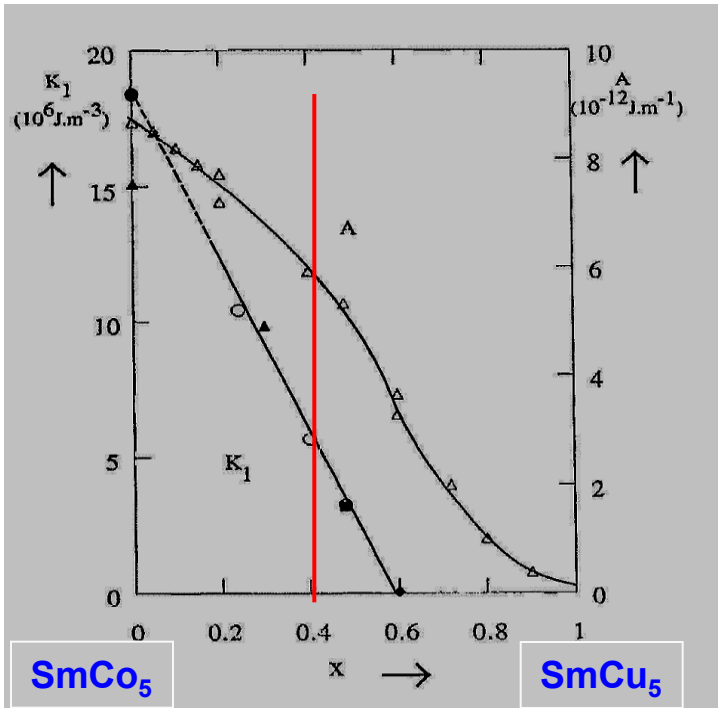

This behavior was connected with coercivity mechanism of the $SmCo_3Cu_2$ phase given by the microstructure [1-2] and diminishing of the intrinsic coercivity by Co substitution with Cu [3].

[1] E. Estevez-Rams, J. Fidler, A. Penton, J.C. Tellez-Blanco, R.S. Turtelli, R. Grossinger, J. Alloys Compounds, 283 (1999) 327.

[2] P. Kerschl, A. Handstein, K. Khlopkov, O. Gutfleisch, D. Eckert, K. Nenkov, J.-C. Te´ llez-Blanco, R. Gro¨ ssinger, K.-H. Mu¨ ller, L. Schultz, J. Magn. Magn. Matter. 290–291 (2005) 420.

[3] E. Lectard, C.H. Allibert, R. Ballou, J. Appl. Phys. 75 (1994) 6277.

The influence of the hard/soft ratio

$SmCo_5$+x% Fe (x=20 or 30),

milled 6 and 8 h and annealed at 550° C for 1.5 h*

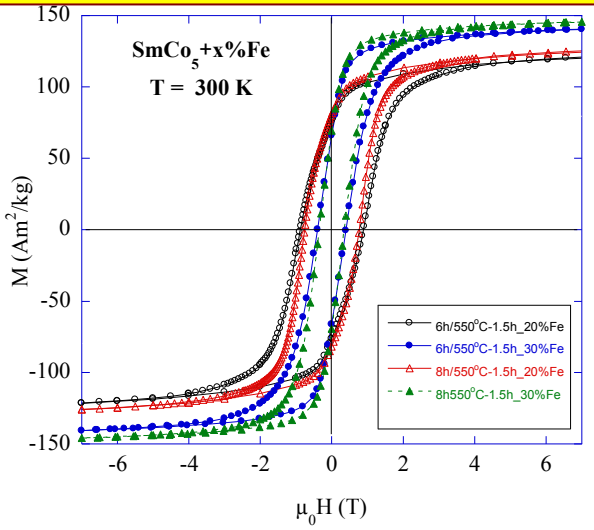

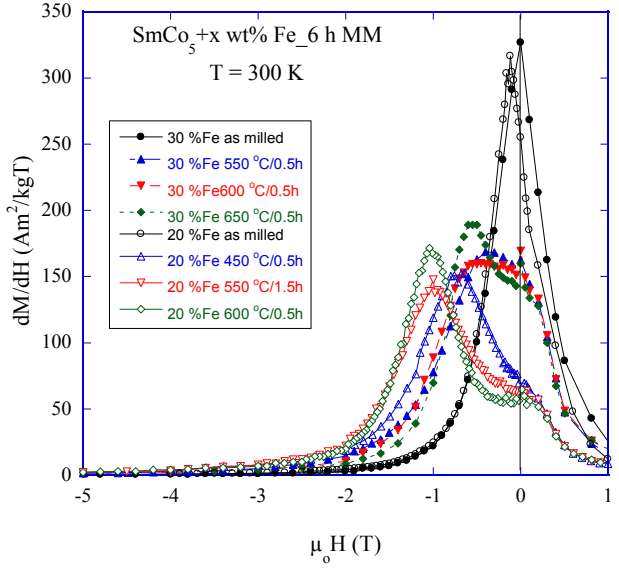

$Nd_2Fe_{14}B$ + 10 % α-Fe; 8h MM

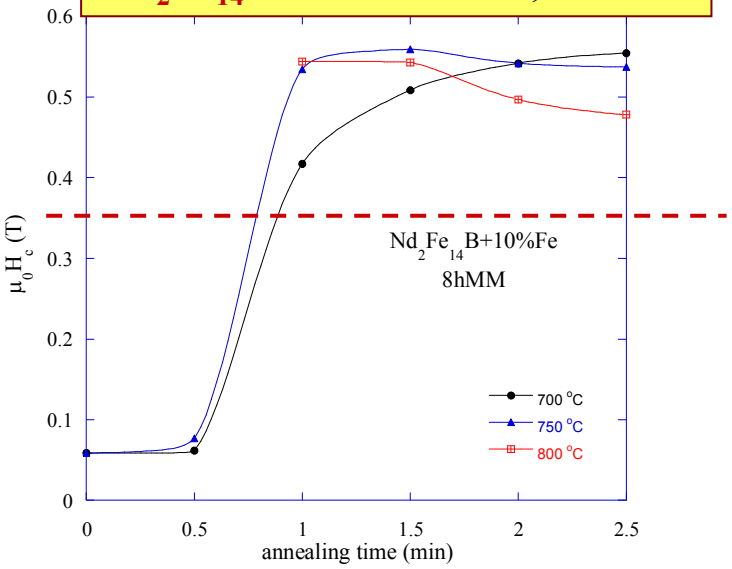

$Nd_2Fe_{14}B$ + 22 % α-Fe; 8h MM

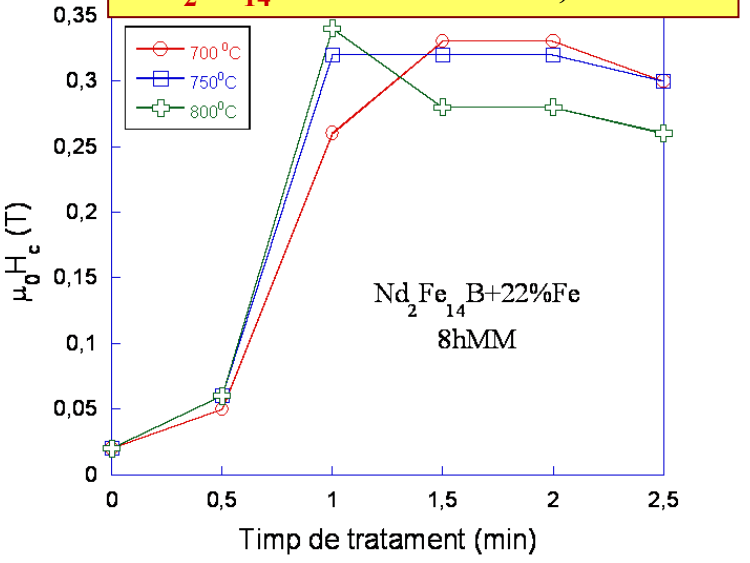

*V. Pop, O. Isnard, D. Givord, I. Chicinas, JMMM 310 (2007) 2489
V. Pop, O. Isnard, D. Givord, I. Chicinas, J. M. Le Breton, JOAM 8 (2006) 494

V. Pop et al., J. Alloys Compd. (2011)
V. Pop et al. , J. Alloys Compd. 581 (2013) 821–827

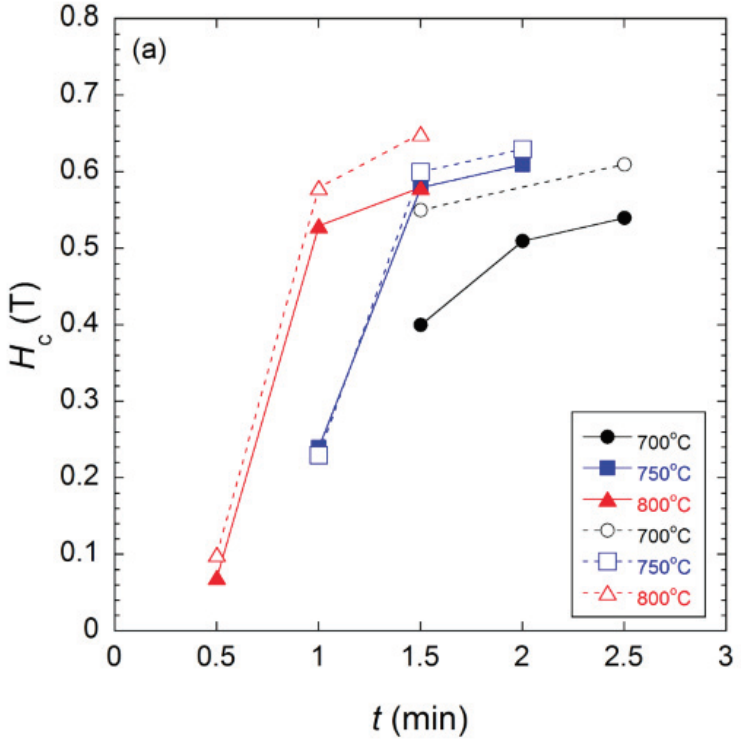

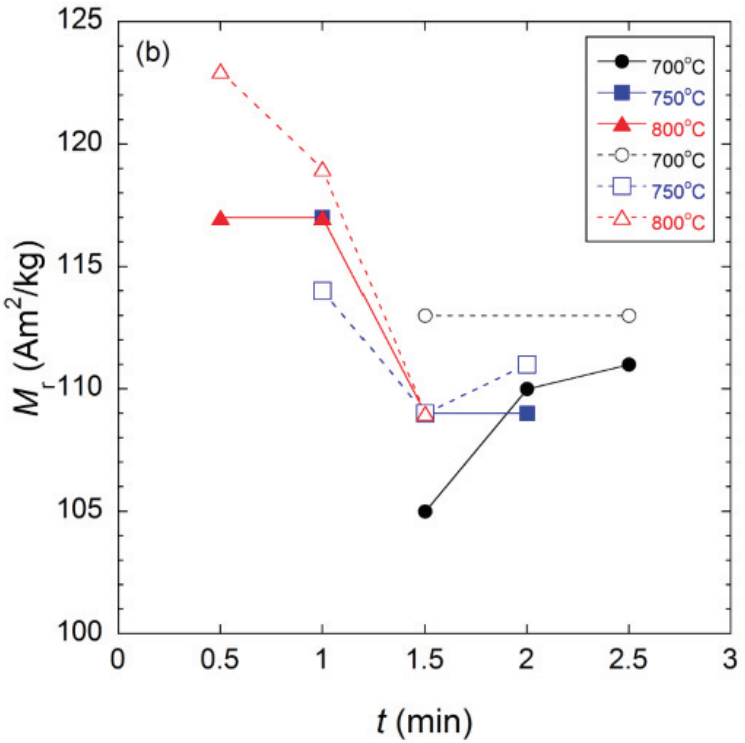

Nd_2Fe1_4B+10 wt% Fe: milled with **Ø = 10 mm** (filled symbols) and **Ø = 15 mm** (empty symbols) balls.

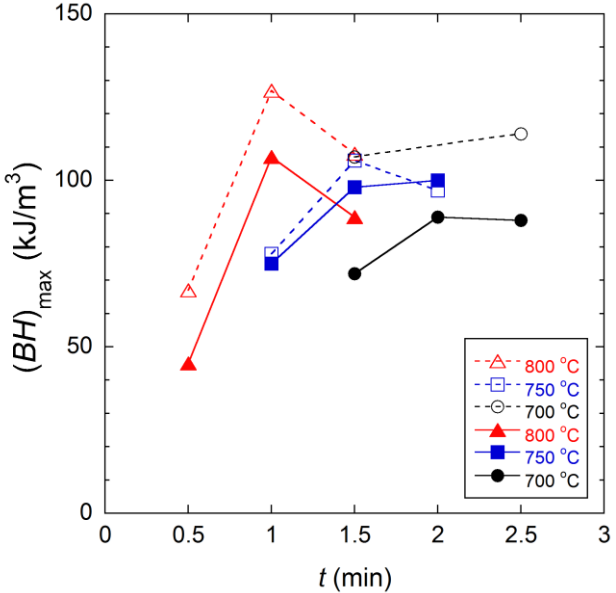

S.Mican, R. Hirian, O. Isnard, I. Chicinaş,
V. Pop, Physics Procedia 75 (2015) 1314

Conclusions

- **MnBi LTP**: large coercivity at high temperature $\Rightarrow$ a good candidate for performance spring magnets
- **MnAl:** stabilisation of τ with conservation of Mn moments
- The ***structure and microstructure*** $\Rightarrow$ strong impact on hard/soft exchange hardness.
- **Intrinsic anisotropy** $\Rightarrow$ the **strength** of the interphase exchange coupling
- ***Annealing*** linked to the ***recrystallisation temperature*** of soft phases and hard magnetic phases; ***recover*** the crystallinity of the hard phase and ***hinder the increase*** of Fe crystallites.
- For ***higher α-Fe concentration*** the magnetic properties are pourer because non correlation with Fe size crystallites.
- The ***short time annealing*** is more appropriate for higher coercivity of the nanocomposites.
- The **geometry and energy of milling** influence the microstructure and the interphase exchange coupling

Prof.dr. Viorel POP	
Prof.dr. Marin Coldea	**intermetallic compounds**
Dr. Diana Benea	**band structure calculation**
Lector dr. Sever Mican	**magnetic materials/thin layers**
Dr. Albert Takacs	**magnetic thin layers**
Drd. Razvan Hirian	**spring magnets**
Drd. Radu Gavrea	**Mn-Al and Heusler compounds**
Stud. Roxana One	**$Fe_{16}N_2$, chemical methods**
Stud. Georgiana Taran	**Mn-Al compounds**
Stud. Akos Ferenczi	**SPS spring magnets**

Prof. dr. Romulus Tetean
Conf.dr. Iosif Deac

- Intermetallic compounds
- Perovskites
- Materials for magnetic refrigeration
- Half metal with 100% theoretical spin polarization
- Manganite : $A_{1-x}B_xMnO_3$
- Cobaltite: $A_{1-x}B_xCoO_3$

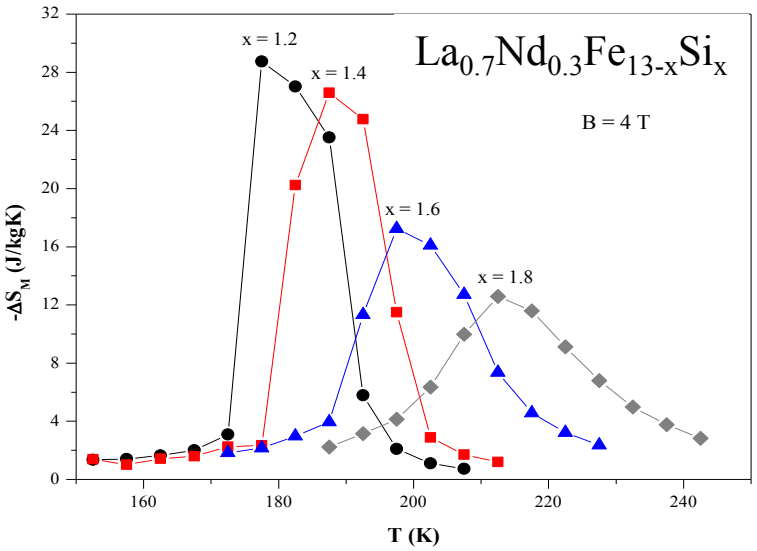

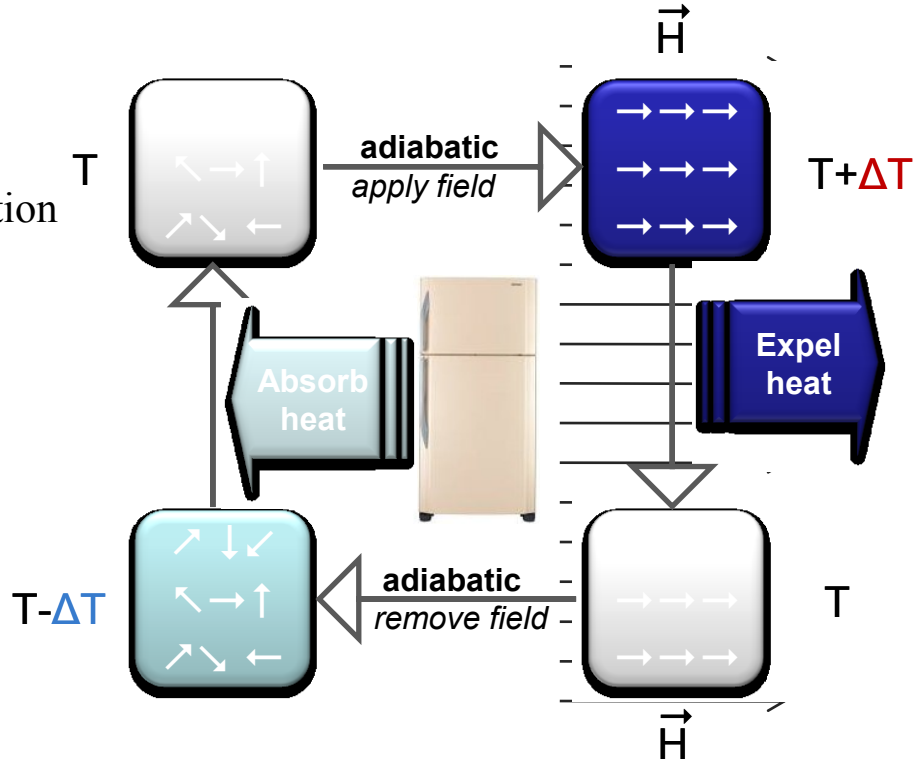

$$S(B,T) = S_{mag}(B,T) + S_{lat}(T) + S_{el}(T)$$

Thank you for your attention

This contribution was supported by the
Romanian Ministry of Education and Research, grant PN-II-ID-PCE-2012-4-0470